NATIONAL AERONAUTICS AND SPACE ADMINISTRATION

Technical Memorandum 33-707

Experimental Determination of the Principal Moments of Inertia of the Helios Prototype Spacecraft

W. H. Gayman

K. Liechti

JET PROPULSION LABORATORY

CALIFORNIA INSTITUTE OF TECHNOLOGY

PASADENA, CALIFORNIA

November 15, 1974

Prepared Under Contract No. NAS 7-100
National Aeronautics and Space Administration

Page intentionally left blank

PREFACE

The work described in this report was performed by the Applied Mechanics Division of the Jet Propulsion Laboratory, as part of the NASA support of the Helios Project.

ACKNOWLEDGMENT

The program of design, test, and analysis described herein is a product of a team effort. Special acknowledgment is due Marc R. Trubert, who supervised the engineering aspects of the program and who made valuable technical suggestions, and to Norman R. Morgan, who "cleared the path" and who, also, made important technical suggestions. The Design Section of the Applied Mechanics Division and the Fabrication Services Division performed superbly in the design and fabrication of the requisite test fixturing under the pressure of severe schedules. The Instrumentation Section of the Applied Mechanics Division also gave excellent support. Finally, the unstinted cooperation of personnel of Messerschmitt-Bölkow-Blohm, GMBH, has been greatly appreciated.

CONTENTS

FIGURES

ABSTRACT

This report presents methods of measuring moments of inertia with very high accuracy.

The moment of inertia of the Helios Spacecraft about its spin axis was determined by use of a "roll-fixture" using two sets of crossed flexure pivots as elastic constraints. The test procedure entailed measurement of a system oscillation period with each of a set of added moment-of-inertia increments. The tare effect of the fixture was determined by a like process and was subtracted from the gross value to yield the spacecraft roll moment of inertia to an estimated accuracy of 0.2%.

"Lateral" moments of inertia (i.e., about each of three axes normal to the spin axis) were determined by a gravity pendulum method that makes use of the fact that any physical pendulum has a minimum period of oscillation determined by a particular distance from the axis of rotation to the system center of gravity. In situations where a knife-edge support is used, this distance is equal to the system centroidal radius of gyration. In the subject tests, the pivoting action was provided by hardened pins rolling on flat ways. The effect of the finite radius of the pins was considered in deriving the equations of motion, from which an error analysis revealed the criterion for maximum accuracy in determining the square of the centroidal radius of gyration.

The swing fixture provided for a number of optional pivot-pin locations giving precisely known distances between successive axes of oscillation. This fixture, with provisions to support the spacecraft, was ballasted to bring its vertical c.g. close to that predicted for the spacecraft. This ballasting was done not because the test method requires an accurate foreknowledge of specimen c.g. position but, rather, to minimize errors in the parallel-axis transfer term while removing the tare of the fixture.

Though the centroidal moment of inertia of the swing fixture was over twice that of the spacecraft, an error analysis showed that accuracies of better than 1.0% were realized for the two lateral principal moments of inertia.

SUMMARY

Principal moments of inertia of the Helios Prototype Spacecraft have been determined at JPL from measurements made during the period, July 2 through July 8, 1974.

Measurements were made with the magnetometer booms installed and in their launch configuration. For measurements of moment of inertia about the roll (spin) axis, the antenna reflector was taped to the spacecraft to lock out "despin" freedom.

Following are the mass properties determined in this program, with estimates of probable errors:

$W = 349.3$ kg ($\pm 0.1\%$ max.)

$\bar{Z} = 929 \pm 19$ mm (above separation plane)

I_{xx}	$= 181.7$ kg $\cdot$ m^2 ($\pm 0.6\%$)	X-Y PLANE (see Fig. 1)
I_{yy}	$= 186.6$ kg $\cdot$ m^2 ($\pm 0.5\%$)	
I_{pp}	$= 188.3$ kg $\cdot$ m^2 ($\pm 0.7\%$)	
I_{max}	$= 188.4$ kg $\cdot$ m^2 ($\pm 0.7\%$)	
I_{min}	$= 179.9$ kg $\cdot$ m^2 ($\pm 0.5\%$)	
I_{zz}	$= 193.9$ kg $\cdot$ m^2 ($\pm 0.2\%$)	

$$\frac{I_{zz}}{(I_{max})_{xy}} = 1.03$$

This report describes the program of test and analysis leading to these results.

INTRODUCTION

This report documents the determination of the principal moments of inertia of the Helios Prototype Spacecraft.

At the outset of the program the following requirements were defined:

An accuracy of 1% in spacecraft moments of inertia was stipulated.

A maximum period of six weeks was available for test planning, fixture design and fabrication, and testing.

The determinations were to be independent of prior estimates of spacecraft inertial properties.

The spacecraft was required to remain vertical, or nearly so.

A consideration of all of these factors, coupled with a review of spacecraft nominal inertial properties as presented in Table 1, led to the choice of a pendulum method for determining radii of gyration about axes in the X-Y centroidal plane and a method using elastic restraint for the determination of the moment of inertia about the Z (roll) axis.

The particular pendulum method selected had been suggested in earlier analytical work as one not requiring prior knowledge or independent measurement of the vertical location of the center of gravity and one having a high accuracy potential. However, it had not been assessed experimentally and so, in conjunction with the primary effort, a scale model program was instituted, as reported in Appendix C.

Common to both methods employed in these tests is the requirement for accurate measurements of mass (M), length (L) and time (T). For the pendulum-method tests, weights were determined by use of precision-calibrated load cells with read-out accuracies to 0.05 kg and probable errors not exceeding 0.02% of full scale. The weight increments used in the roll moment-of-inertia tests were measured on a certified gram balance to the nearest 0.1 gram.

Critical lengths were measured to an accuracy of 0.06%.

Elapsed times for a predetermined number of cycles of oscillation were measured with a photoelectric timing system giving six significant figure read-out.

The influence of these accuracies on the overall accuracy determinations is reported in Appendices A and B.

The following sections of this report deal with the theory, the implementation, the results and the assessments of the determinations of the principal moments of inertia of the Helios Prototype Spacecraft.

DETERMINATION OF THE INERTIA ELLIPSE IN THE X-Y CENTROIDAL PLANE

The Theory

a) Equation of motion

A pendulum method was used to determine moments of inertia of the spacecraft about axes in the X-Y centroidal plane.

Kater's reversible pendulum has been classically used in the determination of the gravitational constant to six significant figures, showing the extreme accuracy obtainable in a pendulum experiment.

The ideal physical pendulum is characterized by its frequency equation.

$$\omega^2 = \frac{g}{D} \tag{1.1}$$

where

ω = circular frequency, radians/sec.

g = gravitational constant, m/sec^2.

D = distance, in meters, from the center of rotation to the "center of oscillation," also referred to as the "center of percussion."

The parameter, D, is recognized as the length, L, of an equivalent simple pendulum. It is given by

$$D = \frac{r^2 + \rho_o^2}{r} \tag{1.2}$$

where ρ_o is the centroidal radius of gyration and r is the distance from the pivot point to the center of gravity (c.g.). D has a minimum and, consequently, the frequency of oscillation has a maximum for $r = \rho_o$. An error analysis shows that the maximum accuracy in the determination of ρ_o^2 exists also for $r = \rho_o$.

In a test situation axes of oscillation are commonly realized with knife-edge pivots. In dealing with massive systems, the knife-edge design poses the materials problems of galling and fretting under bearing stresses. Accordingly, an alternative is used in which the pivot system is comprised of finite-diameter pins rolling on flat ways. While this system provides a reduction in bearing stresses, it also poses some readjustments in the equations of motion, as the "rest point" now describes cycloidal motions under angular oscillations.

Figure 2 shows the geometry of such a system, in which

a = radius of pin

r = distance from pin support to the system c.g.

θ = angular amplitude of displacement

x = horizontal displacement of system c.g.

z = vertical displacement of system c.g.

m = system mass

ρ_o = system centroidal radius of gyration

For a small angular displacement, θ (assuming no slippage of the pin on its support), the horizontal displacement of the c.g. is

$$x = (r + a)\theta - a\theta - a(\theta - \sin\theta) \tag{1.4}$$

or, to a first approximation,

$$x \approx r\theta - a\frac{\theta^3}{6} \tag{1.5}$$

The associated vertical displacement is

$$\begin{aligned} z &= (r + a)(1 - \cos\theta) \\ &\approx (r + a)\frac{\theta^2}{2} \end{aligned} \tag{1.6}$$

The kinetic energy of this system is

$$T = \frac{1}{2}mv^2 + \frac{1}{2}m\rho_o^2\dot{\theta}^2 \tag{1.7}$$

where

$$v^2 = \dot{x}^2 + \dot{z}^2 \tag{1.8}$$

Use of Eqs. 1.5, 1.6, and 1.8 in Eq. 1.7 leads to

$$T = \frac{1}{2}I\dot{\theta}^2 + \text{higher order terms in } \dot{\theta} \tag{1.9}$$

where

$$I = m\left(r^2 + \rho_o^2\right) \tag{1.10}$$

Neglecting the higher order terms leads to the inertia moment,

$$\frac{d}{dt}\left(\frac{\partial T}{\partial \dot{\theta}}\right) = I\ddot{\theta} \tag{1.11}$$

The potential energy of the system is (for small amplitudes)

$$\begin{aligned} V &= mgz \\ &\approx mg\,(r + a)\frac{\theta^2}{2} \end{aligned} \tag{1.12}$$

The restoring moment is

$$\frac{\partial V}{\partial \theta} = mg\,(r + a)\theta \tag{1.13}$$

The equation of motion without external forcing and neglecting damping is:

$$I\ddot{\theta} + mg\,(r + a)\theta = 0 \tag{1.14}$$

For simple harmonic motion,

$$\theta = \theta_o e^{i\omega t}$$

$$\ddot{\theta} = -\omega^2\theta$$

Thus

$$\omega^2 = \left(\frac{r + a}{r^2 + \rho_o^2}\right) g \tag{1.15}$$

Let

$$D \equiv \frac{r^2 + \rho_o^2}{r + a} \tag{1.16}$$

Then

$$\omega^2 = \frac{g}{D} \tag{1.1}$$

or

$$T^2 = \frac{4\pi^2}{g} D$$

where T is the period of oscillation in seconds.

It is significant to note that the pin radius, a, enters only into the potential energy relation of Eq. (1.12); it does not appear in the kinetic energy relations (Eqs. 1.9 and 1.10) because the instantaneous center of rotation remains at the interface between pin and support.

The method used to determine ρ_o^2 was to perform measurements of the period of oscillation for several locations of the axis of oscillation (i.e., several values of r) in a search for the minimum period, T_m, and, correspondingly, a minimum value of D.

b) Determination of ρ_o^2 from a minimum of D

In Eq. (1.16), let r + a = R, so that

$$r = R - a \tag{1.17}$$

Substituting of Eq. (1.17) into Eq. (1.16) leads to

$$D = R - 2a + \frac{\rho_o^2 + a^2}{R} \tag{1.18}$$

For the minimum sensitivity of D with respect to R, i.e.,

$$\frac{dD}{dR} = 0$$

we have

$$R = \sqrt{\rho_o^2 + a^2} \tag{1.19}$$

Substitution of Eq. (1.19) into Eq. (1.18) leads to a minimum value,

$$D_m = 2\left(\sqrt{\rho_o^2 + a^2} - a\right)$$

from which

$$\rho_o^2 = \left(\frac{D_m}{2}\right)^2 \left(1 + \frac{4a}{D_m}\right) \tag{1.20}$$

c) Determination of ρ_o^2 from a best-fit curve of period vs pivot pin location.

The square of the radius of gyration, ρ_o^2, can also be determined from a best fit, in a least-squares sense, of the test data, i.e., the oscillation periods, T_i, as a function of the oscillation axis locations, r_i.

$$\rho_o^2 = \frac{1}{n}\left[\sum_{i=1}^{n} (r_i + a)\frac{g}{4\pi^2} T_i^2 - \sum_{i=1}^{n} r_i^2\right] \tag{1.21}$$

where n is the number of axis locations as shown in Appendix A.

d) Error in ρ_o^2 from a minimum in period of oscillation

Differentiating Eq. (1.20) gives

$$\frac{d\rho_o^2}{\rho_o^2} = \left(2 - \frac{D_m a}{\rho_o^2}\right)\frac{dD_m}{D_m} + \left(\frac{D_m a}{\rho_o^2}\right)\frac{da}{a}$$

Eq. (1.1) may be written in the form,

$$D_m = \frac{g}{4\pi^2} T_m^2 \tag{1.22}$$

where T_m is the minimum period of oscillation.

$$\frac{dD_m}{D_m} = \frac{1}{D_m}\left(\frac{\partial D_m}{\partial g}\right) dg + \frac{1}{D_m}\left(\frac{\partial D_m}{\partial T_m}\right) dT_m$$

$$\frac{\partial D_m}{\partial g} = \frac{T_m^2}{4\pi^2} = \frac{D_m}{g}$$

$$\frac{\partial D_m}{\partial T_m} = \frac{2gT_m}{4\pi^2} = \frac{2D_m}{T_m}$$

Thus

$$\frac{dD_m}{D_m} = \frac{dg}{g} + 2\frac{dT_m}{T_m}$$

and

$$\frac{\Delta\rho_o^2}{\rho_o^2} = \left(2 - \frac{agT_m^2}{4\pi^2\rho_o^2}\right)\left(\frac{\Delta g}{g} + 2\frac{\Delta T_m}{T_m}\right) + \frac{agT_m^2}{4\pi^2\rho_o^2}\left(\frac{\Delta a}{a}\right) \tag{1.23}$$

In the special case of the knife-edge pivot (a = 0), Eq. (1.23) reduces to

$$\frac{\Delta\rho_o^2}{\rho_o^2} = 2\frac{\Delta g}{g} + 4\frac{\Delta T_m}{T_m} \tag{1.24}$$

The error in ρ_o^2 is not explicitly related to the radial distance, r. This makes the determination of ρ_o^2 independent of the center of gravity to the first order of approximation.

Once ρ_o^2 has been obtained, the radial distance, r, from the system c.g. to the pivot point associated with T_m may be determined from Eqs. (1.17) and (1.19).

e) Error on ρ_o^2 from a best-fit curve of period vs. pivot pin location

Appendix A presents a statistical error analysis based on the best-fit curve. An estimate for the mean square error is (Appendix A, Eq. A-18)

$$S^2 = \frac{1}{n-1} \sum_{i=1}^{i=n} \left[\rho_o^2 - (r_i + a) \frac{g}{4\pi^2} T_i^2 + r_i^2 \right]^2$$

Test Implementation

a) Setup

A support cradle accommodating a spacecraft adapter is shown in Fig. 3. The box section supporting the adapter was designed for high torsional stiffness; even though the inertia torques imposed during oscillation were calculated to be quite low, the associated angular deflections between sidearms were held to very small values (less than 0.00001 rad.) to limit periodic vertical migration of the instantaneous center of rotation to less than 1 mm with peak amplitudes of oscillation less than 1 deg.

Likewise, the sidearms carrying the support pins were designed for high stiffness in the plane of oscillation.

The bare cradle was provided with ballast weights, based on mass property calculations, to raise the center of gravity of the cradle assembly (plus adapter and V-band) close to the nominal vertical c.g. of the spacecraft in order to minimize the transfer term as seen from Eq. (1.27). These ballast weights also provided a series of precisely spaced holes into which the pivot pins could be inserted. (See Fig. 4.)

Hardened and ground bearing plates, bolted to support stands, provided for rolling contact in the cradle suspension.

A specially-designed hoisting sling suspended from a bridge crane was used to lift the entire assembly during the operations of weighing and of changing pin positions.

Prior to installing the adapter on the cradle, the test system was proof-loaded with a dead weight of 1360 kg.

After installation of the adapter and V-band, the carriage assembly was weighed by use of a precisely calibrated load cell between the crane hook and the hoisting sling. The tare weight of the hoisting sling was also recorded.

The vertical position of the c.g. of the cradle assembly was determined by measurement of the static moment required to rotate the assembly through 90 deg. Accuracy of the angle of rotation was determined by a Hilger and Watts inclinometer giving a vernier reading to the nearest minute of arc.

The data obtained from these static measurements of cradle weight and c.g. determination are reported below, under Test Results. An error analysis is presented in Appendix A.

Mechanical stops were provided to prevent cradle rotation during installation of the spacecraft. Following spacecraft installation, the weight of the entire assembly was determined. Views of the Helios spacecraft on the test fixture are shown in Figs. 5 and 6.

b) Tests

There were four series of oscillation tests conducted. One of these was to determine the centroidal radius of gyration of the fixture alone. The remaining three included the spacecraft with oscillations about the x, y, and p[1] axes, respectively. Each series was repeated at least once to evaluate reproducibility.

The following features were common to all of these tests. The photoelectric sensor was positioned under one end of the cradle platform, which carried a plate that interrupted the light beam twice per oscillation (Fig. 7). With the cradle at rest, the sensor was placed so that the electronic counter/timer (Fig. 8) was on the verge of tripping. (The resolution in manual placement is estimated to be about 1.5 mm. The associated error ascribable to damping of amplitude over the elapsed time for 40 cycles of oscillation is estimated to be less than 0.002%.)

In each test series, timings were made with five different (parallel) axes of rotation by use of five consecutive hole positions for the pivot pins.

---

[1]The "p" axis is rotated 33.75° from the +y axis toward the +x axis.

The positioning of these pin locations in relation to the spacecraft separation plane is shown in Fig. 9. With each pivot axis, two measurements were made of the elapsed time (for 40 cycles of oscillation) with an initial amplitude at the sensor of about 25 mm, and another two were made with an initial amplitude of about 13 mm. An amplitude effect on elapsed time was discernable and the times for "zero amplitude" were obtained by graphical extrapolation. In this way external aerodynamic effects and small nonlinearities in kinematic behavior have been essentially eliminated.

One deficiency of the fixturing is to be noted. Each bearing plate on which the support pins rolled was canted because of warpage in welding its faceplate to the central column. Pressure of time precluded correcting this situation by a final machining, and the result was that each pin did not have line contact, but, rather, bore on one edge. This resulted in progressive galling of the pins, which subsequent Rockwell tests have shown were not as hard as the bearing plates. In future tests of a similar nature, this problem would be eliminated.

Test Results

a) Configuration 1, cradle plus adapter and V-band:

Weight (including hoisting sling)	469.7 kg
Tare of hoisting sling	51.9 kg
Net, cradle plus adapter and V-band	417.7 kg

C.G. determination[2]

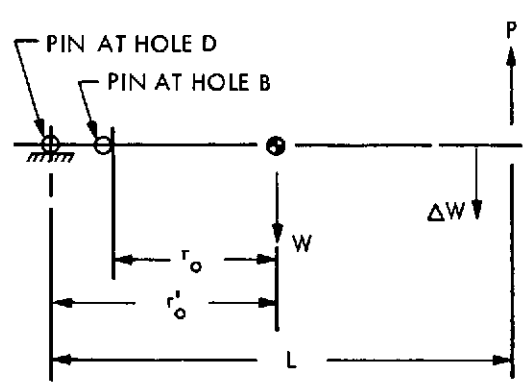

[2]The V-band was not available at the time of these measurements. Its effects are accounted for in the following calculations.

$$P_{net} = 186.7 \text{ kg (less V-band)}$$

$$W_{tot} = 417.7 \text{ kg (including V-band)}$$

$$L = 2.169 \text{ m}$$

$$\Delta W = 7.54 \text{ kg @} L' = 2.040 \text{ m (V-band)}$$

The static moment about the center of pin D is

$$M = W_{tot}\, r_o' - (PL + \Delta W L') = 0$$

$$r_o' = \frac{PL + \Delta W L'}{W_{tot}}$$

$$r_o' = 1.0064 \text{ m}$$

From the base of pin B,

$$r_o = r_o' - 0.1022$$

$$r_o = 0.9042 \text{ m}$$

b) Configurations 2, 3, 4, cradle plus spacecraft:

Weight (including hoisting sling)	820.1 kg
Tare of hoisting sling + load cell cable	53.0
Net, cradle plus spacecraft	767.1 kg
Cradle plus adapter and V-band	417.7
Net, Spacecraft	349.3 kg

c) Timing measurements, all configurations

The results of the timing measurements are presented in Tables 2 through 5.

Data Processing

By gravimetric measurements conducted by the Caltech Seismological Laboratory, the gravitational constant on the ground floor of JPL's Gyro Laboratory has been established as

$$g = 9.79543 \text{ m/sec}^2$$

In consideration of the small elevation difference between the Gyro Lab and the site of the subject tests (Bldg. 144), the value listed above has been used, rounded off to five significant figures.

Appendix A makes use of the test data presented in Tables 2 through 5 to obtain, through an iterative process, the "least squares" best fit of discrete data points to the theoretical relationships. Here, r is replaced by $r_o + x_i$, where, as used, r_o is the distance from the base of the pivot pin at Hole B to the system vertical c.g. position. This process requires initial estimates of r_o and ρ_o^2 for each data set. These initial estimates were obtained from plots of oscillation period, T vs x. The minimum time, T_m, obtained for each configuration from a visually-faired curve was used in Eqs. (1.22) and (1.20) to obtain a trial value of ρ_o^2. The value of x at which this minimum appeared was used to obtain the trial value of r_o.

The initial statistical curve fitting reported in Appendix A has been used primarily to obtain improved values of r_o. These, of course, should be identical, regardless of the spacecraft orientation on the cradle. However, there were differences in the three values of r_o with the spacecraft x, y, and p axes parallel to the oscillation axis, although the maximum difference from the average was only 0.7%. A "consistent" average value of r_o for the three axes was chosen for the final calculations of ρ_o^2 for each test value of x_i. These values were used in a least-squares best fit, Eq. (1.21), to the linear relationship, ρ_o^2 = a constant, for each spacecraft orientation. Additionally, the variance has been calculated to obtain a most probable error in each value of ρ_o^2.

The results of the processing of the data for the fixture only and for the fixture plus spacecraft in each of the three orientations are presented in Table 6. Results of the final calculations are presented graphically in Figs. 10a through 10d as plots of T vs. x. Here, the test points are circled and the theoretical best fits are shown as solid lines. The results are also shown in Figs. 11a through 11d wherein the dashed lines represent the statistically derived values of ρ_o^2, showing that the dispersion from the mean is random with, as expected, no apparent correlation between ρ_o^2 and the location of the axis of oscillation.

a) Separation of spacecraft and fixture

To obtain the desired mass properties of the spacecraft (subscript S), the effects of the fixture (subscript F) must be removed from the total (subscript T).

Letting M, r_o, and ρ_o represent mass, c.g. coordinate, and radius of gyration, respectively, there exists, for static equilibrium, the relation

$$M_F (r_{oT} - r_{oF}) + M_S (r_{oT} - r_{oS}) = 0$$

from which

$$r_{oT} - r_{oS} = -\frac{M_F}{M_S} (r_{oT} - r_{oF}) \tag{1.25}$$

also, the total moment of inertia is

$$(M_F + M_S) \rho_{oT}^2 = M_F \rho_{oF}^2 + M_F (r_{oT} - r_{oF})^2 + M_S \rho_{oS}^2 + M_S (r_{oT} - r_{oS})^2 \tag{1.26}$$

From Eqs. (1.25) and (1.26), there follows,

$$\rho_{oS}^2 = \left(1 + \frac{M_F}{M_S}\right) \rho_{oT}^2 - \frac{M_F}{M_S} \rho_{oF}^2 - (r_{oT} - r_{oF})^2 \frac{M_F}{M_S} \left(1 + \frac{M_F}{M_S}\right) \tag{1.27}$$

Because of the fixture ballast weights, $r_{oT} - r_{oF}$ is very small (cf. Table 6), and the last term may be neglected.

Calculations of the variances on ρ_{oS}^2 are presented in Appendix A, together with moments of inertia about the x, y, and p axes and their associated probable errors. These results are listed in the Summary.

b) The inertia ellipse

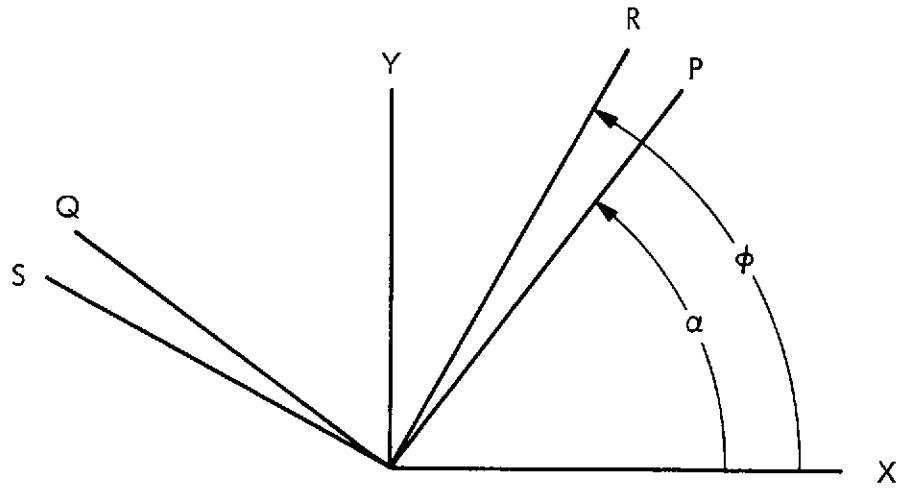

$$I_p = I_x \cos^2 \alpha + I_y \sin^2 \alpha - U_{xy} \sin 2\alpha \qquad (1.28)$$

where U_{xy} = product of inertia about the x and y axes. From Eq. (1.28),

$$U_{xy} = \frac{I_x \cos^2 \alpha + I_y \sin^2 \alpha - I_p}{\sin 2\alpha} \qquad (1.29)$$

Also, for other orthogonal axes, r and s,

$$U_{rs} = \frac{1}{2}(I_x - I_y) \sin 2\phi + U_{xy} \cos 2\phi \qquad (1.30)$$

where ϕ is the angle between the r and x axes. For the r and s axes to be principal axes, $U_{rs} = 0$, and

$$\tan 2\phi = \frac{-2U_{xy}}{I_x - I_y} \qquad (1.31)$$

The procedure, here, is straightforward. U_{xy} is calculated by use of Eq. (1.29) for obtaining ϕ by Eq. (1.31). Then Equation (1.28) is used,

with ϕ replacing α, to obtain the principal moments of inertia. An error analysis is given in Appendix A.

Here,

$$I_x = 181.69 \text{ kg} \cdot \text{m}^2$$
$$I_y = 186.57 \text{ kg} \cdot \text{m}^2$$
$$I_p = 188.27 \text{ kg} \cdot \text{m}^2$$

$$\alpha = 56.25° \text{ (counterclockwise from +X axis)}$$

from which ϕ can be calculated.

$$\phi = 27.445° = 0.4790 \text{ rad.}$$

Then from Eq. (1.28), with ϕ replacing α,

$$I_r = 188.37 \text{ kg} \cdot \text{m}^2 = I_{max}$$

and

$$I_s = I_x + I_y - I_r = I_{min}$$
$$= 179.88 \text{ kg} \cdot \text{m}^2$$

These results are listed in the Summary.

DETERMINATION OF THE MOMENT OF INERTIA ABOUT THE Z (ROLL) AXIS

Measurement Concept

For a body in free sinusoidal oscillation about a fixed axis, the period of oscillation, T_o is determinable from the relation,

$$\omega_o^2 \equiv \frac{4\pi^2}{T_o^2} = \frac{K}{I_o} \qquad (2.1)$$

where K is the restoring moment per radian angular displacement and I_o is the moment of inertia of the body.

If an increment, ΔI of the moment of inertia I_o, is added to the system, the new period, T, is obtained from

$$\frac{4\pi^2}{T^2} = \frac{K}{I_o + \Delta I} \tag{2.2}$$

Dividing Eq. (2.1) by Eq. (2.2) leads to

$$T^2 = T_o^2 + \left(\frac{T_o^2}{I_o}\right)\Delta I \tag{2.3}$$

Thus the square of the period is a linear function of ΔI in which the slope m is:

$$m = \frac{T_o^2}{I_o} \tag{2.4}$$

Thus

$$I_o = \frac{T_o^2}{m} \tag{2.5}$$

This approach, which has been in occasional use, entails merely the precise determination of several ΔI's and the associated periods of oscillation from which to establish the slope, m, and thus I_o from Eq. (2.5).

Test Implementation

The easiest implementation of the concept is to use elastic restoring torque. Accordingly, a test fixture was designed to employ two vertically separated sets of crossed flexure pivots between a floor-mounted support stand and the rotational table. This fixture, shown in Fig. 12, carries a long transverse arm with provisions for attaching weight increments.

The flexures were designed to withstand the dead load of the spacecraft and the bending stresses due to maximum oscillation amplitudes with an ample margin of safety. The lower pair of flexures is shown in Fig. 13.

Prior to installation of the spacecraft adapter on the rotational table, the system was proof-loaded with a dead weight of 1360 kg, and oscillated through the design amplitude while under load.

A test was also made to ascertain that the axis of table rotation was actually on the spacecraft roll axis as established by the adapter position.

With the spacecraft adapter and V-band in place, tests were made to determine the moment of inertia of the fixture. The spacecraft was then installed, and timing measurements of the complete system were made. Figs. 14 and 15 show the spacecraft in position on the test fixture.

Fig. 16 shows the placement of the photoelectric timing system and four of the weight increments secured near the end of the transverse arm at a precisely determined distance from the roll axis.

Test Results

The data obtained in these tests are presented numerically in Tables 7 and 8 and graphically in Figs. 17 and 18.

Data Processing

The test data of Tables 7 and 8 have been used in a statistical analysis presented in Appendix B to derive the roll moments of inertia of the fixture and the spacecraft plus fixture, and the statistical variances on each. The results are presented in Table 9.

CONCLUSIONS

The two test methods used for obtaining principal moments of inertia are deemed wholly satisfactory. The probable errors in spacecraft principal moments of inertia are below the target values of one percent set at the beginning of the program in spite of the large tare moment of inertia that had

to be accepted in the pendulous tests. The test hardware provided sufficiently low damping (damping coefficient, $\gamma < 0.01\%$) that errors in elapsed times of oscillation contributed negligibly to overall error.

Although the results are excellent, the full accuracy potential of the multiaxis, pendulous method employed here was not completely realized because of alignment and material deficiencies local to the support pins and their bearing plates. Correction of these deficiencies is expected to lead to an accuracy much better than one percent.

The error analysis of vertical c.g. determination (Appendix A) indicates that the chosen pendulous method of determining ρ_o^2 is not a precise method of locating center of gravity. Nor should it be. By intent, the test parameters were chosen to place minimal dependence on knowledge or determination of c.g. position:

$$\frac{dD}{dr} = 0$$

The minimum of "D," or of period of oscillation, is much more precisely bounded than is the value of "r" at which this minimum occurs.

Table 1. Helios prototype spacecraft mass property estimates provided by Messerschmitt-Bölkow - Blohm, GMBH (Tentative information)

W	= 358 kg
$\bar{Z}$	= 980 mm (above separation plane)
I_{ox}	= 165 kg · m^2
I_{oy}	= 157 kg · m^2
I_{oz}	= 192 kg · m^2

Table 2. Timing measurements for fixture plus adapter and V-band

Hole Designation	x mm	Initial Amplitude mm	Elapsed Time for 40 Cycles sec.	Period, T, at "Zero Amplitude" sec.
B	0	25	113.739	
		25	113.738	
		13	113.727	
		13	113.725	
		0	113.720	2.8430
B (repeat)		25	113.724	
		25	113.718	
		13	113.706	
		13	113.707	
		0	113.700	2.8425
C	43.18	25	113.608	
		25	113.605	
		13	113.592	
		13	113.593	
		0	113.585	2.8396
C (repeat)		25	113.588	
		25	113.582	
		13	113.593	
		13	113.592	
		0	113.595	2.8399
D	86.36	25	113.572	
		25	113.570	
		13	113.567	
		13	113.562	
		0	113.560	2.8390
D (repeat)		25	113.541	
		25	113.540	
		13	113.531	
		13	113.534	
		0	113.532	2.8383
E	128.0	25	113.563	
		25	113.566	
		13	113.555	
		13	113.556	
		0	113.552	2.8388

Table 2 (contd)

Hole Designation	x mm	Initial Amplitude mm	Elapsed Time for 40 Cycles sec.	Period, T, at "Zero Amplitude" sec.
E (repeat)		25	113.604	
		25	113.600	
		13	113.590	
		13	113.591	
		0	113.586	2.8397
F	166.9	25	113.697	
		25	113.698	
		13	113.682	
		13	113.683	
		0	113.678	2.8420
F (repeat)		25	113.722	
		25	113.718	
		13	113.716	
		13	113.714	
		0	113.714	2.8429

Initial estimates for statistical determinations:

$\rho_o^2 = 1.035\ m^2$ $\qquad r_o = 0.925\ m$

Table 3. Timing measurements for fixture plus spacecraft Oscillation about S/C x-x axes

Hole Designation	x mm	Initial Amplitude mm	Elapsed Time sec.	Period, T, at "Zero Amplitude" sec.
D	86.36	25	106.879	
		25	106.878	
		13	106.865	
		13	106.872	
		0	106.865	2.6716
D (repeat)		25	106.860	
		25	106.858	
		13	106.840	
		13	106.843	
		0	106.835	2.6709
C	43.18	25	106.607	
		25	106.594	
		13	106.593	
		13	106.595	
		0	106.592	2.6648
C (repeat)		25	106.544	
		25	106.539	
		13	106.528	
		13	106.525	
		0	106.522	2.6631
B	0	25	106.376	
		25	106.374	
		13	106.340	
		13	106.342	
		0	106.328	2.6582
B (repeat)		25	106.417	
		25	106.425	
		13	106.403	
		13	106.400	
		0	106.387	2.6597
B (repeat)		25	106.429	
		25	106.425	
		13	106.419	
		13	106.419	
		0	106.413	2.6603

Table 3 (contd)

Hole Designation	x mm	Initial Amplitude mm	Elapsed Time sec.	Period, T, at "Zero Amplitude" sec.
A	-43.18	25	106.440	
		25	106.434	
		13	106.408	
		13	106.414	
		0	106.395	2.6599
A (repeat)		25	106.392	
		25	106.391	
		13	106.381	
		13	106.382	
		0	106.379	2.6595
J	-91.31	25	106.568	
		25	106.566	
		13	106.549	
		13	106.547	
		0	106.540	2.6635
J (repeat)		25	106.509	
		25	106.512	
		13	106.489	
		13	106.489	
		0	106.476	2.6619
J (repeat)		25	106.531	
		25	106.521	
		13	106.494	
		13	106.497	
		0	106.480	2.6620

Initial estimates for statistical determinations:

$$\rho_o^2 = 0.8010\ m^2 \qquad r_o = 0.905\ m$$

Table 4. Timing measurements for fixture plus spacecraft oscillation about S/C y-y axes

Hole Designation	x mm	Initial Amplitude mm	Elapsed Time for 40 Cycles sec.	Period, T, at "Zero Amplitude" sec.
D	86.36	25	106.986	
		25	106.980	
		13	106.965	
		13	106.960	
		0	106.955	2.6739
D (repeat)		25	106.987	
		25	106.982	
		13	106.956	
		13	106.962	
		0	106.944	2.6736
C	43.18	25	106.762	
		25	106.761	
		13	106.743	
		13	106.741	
		0	106.727	2.6682
C (repeat)		25	106.808	
		25	106.809	
		13	106.789	
		13	106.785	
		0	106.779	2.6695
B	0	25	106.636	
		25	106.644	
		13	106.627	
		13	106.625	
		0	106.620	2.6655
B (repeat)		25	106.595	
		25	106.586	
		13	106.567	
		13	106.570	
		0	106.558	2.6640
B (repeat)		25	106.663	
		25	106.636	
		13	106.612	
		13	106.609	
		0	106.589	2.6647

Table 4 (contd)

Hole Designation	x mm	Initial Amplitude mm	Elapsed Time for 40 Cycles sec.	Period, T, at "Zero Amplitude" sec.
A	-43.18	25	106.678	
		25	106.676	
		13	106.646	
		13	106.645	
		0	106.635	2.6659
A (repeat)		25	106.647	
		25	106.648	
		13	106.632	
		13	106.638	
		0	106.634	2.6659
J	-91.31	25	106.783	
		25	106.782	
		13	106.765	
		13	106.758	
		0	106.753	2.6688
J (repeat)		25	106.849	
		25	106.841	
		13	106.827	
		13	106.829	
		0	106.820	2.6705

Initial estimates for statistical determinations:

$\rho_o^2 = 0.8079\ m^2$ $\qquad r_o = 0.9035\ m$

Table 5. Timing measurements for fixture plus spacecraft oscillation about S/C p-p axes

Hole Designation	x mm	Initial Amplitude mm	Elapsed Time sec.	Period, T, at "Zero Amplitude" sec.
D	86.36	25	107.107	
		25	107.102	
		13	107.080	
		13	107.082	
		0	107.070	2.6768
D (rerun)		25	107.089	
		25	107.096	
		13	107.089	
		13	107.090	
		0	107.090	2.6773
C	43.18	25	106.810	
		25	106.804	
		13	106.789	
		13	106.784	
		0	106.779	2.6695
C (repeat)		25	106.870	
		25	106.861	
		13	106.848	
		13	106.848	
		0	106.840	2.6710
B	0	25	106.699	
		25	106.691	
		13	106.682	
		13	106.682	
		0	106.676	2.6669
B (repeat)		25	106.723	
		25	106.724	
		13	106.704	
		13	106.707	
		0	106.698	2.6675
A	-43.18	25	106.759	
		25	106.760	
		13	106.754	
		13	106.751	
		0	106.752	2.6688

Table 5 (contd)

Hole Designation	x mm	Initial Amplitude mm	Elapsed Time sec.	Period, T, at "Zero Amplitude" sec.
		25	106.722	
		25	106.712	
		13	106.708	
		13	106.712	
		0	106.707	2.6677
J	-91.31	25	106.864	
		25	106.850	
		13	106.831	
		13	106.830	
		0	106.820	2.6705
J (repeat)		25	106.892	
		25	106.884	
		13	106.860	
		13	106.864	
		0	106.852	2.6713

Initial estimates for statistical determinations:

$\rho_o^2 = 0.8097\ m^2$ $\qquad r_o = 0.9042\ m$

Table 6. Processed results of oscillation tests

Fixture plus adapter and V-band		
	Best Fit	Based on Static-Test
r_o (m)	0.9161	0.9042
ρ_o^2 (m^2)	1.0296	1.0297
$\Delta\rho_o^2/\rho_o^2$	0.17%	0.17%
Δr_o (mm) best fit and static test	11.9	

Fixture plus spacecraft			
	Axis	Best Fit	Consistent C.G.
X-X	r_o (m)	0.9131	0.9065
	ρ_o^2 (m^2)	0.7972	0.7976
	$\Delta\rho_o^2/\rho_o^2$	0.16%	0.16%
Y-Y	r_o (m)	0.9016	0.9065
	ρ_o^2 (m^2)	0.8040	0.8038
	$\Delta\rho_o^2/\rho_o^2$	0.19%	0.11%
P-P	r_o (m)	0.9049	0.9065
	ρ_o^2 (m^2)	0.8061	0.8060
	$\Delta\rho_o^2/\rho_o^2$	0.19%	0.19%
	r_o (mm) average	906.5	
	Δr_o (mm) maximum deviation	6.6	
	Δr_o (mm) standard deviation	5.2	

Table 7. Timing measurements for bare fixture plus adapter and V-band oscillation about S/C roll axis (initial amplitude, $\theta_o = 0.016$ rad.)

ΔI $kg \cdot m^2$	Elapsed Time for 80 Cycles sec.	Average Period, T, sec.	T^2 $(sec.)^2$
0	144.872 144.873	1.81090	3.2794
1.0192	145.818 145.813	1.82270	3.3223
2.0380	146.761 146.758	1.83450	3.3654
3.0575	147.684 147.684	1.84605	3.4079
4.0765	148.623 148.633	1.85784	3.4516
5.0961	149.555 149.562	1.86949	3.4950

Table 8. Timing measurements for fixture plus spacecraft oscillation about S/C roll axis (initial amplitude, θ_o = 0.016 rad.)

ΔI kg · m^2	Elapsed Time for 80 Cycles sec.	Average Period, T, sec.	T^2 $(sec.)^2$
0	270.671		
	270.666	3.38336	11.4471
4.7407	273.013		
	273.017	3.42169	11.6464
9.4801	275.355		
	275.370	3.44204	11.8476
	275.301		
	275.324	3.44141	11.8433
14.219	277.644		
	277.673	3.47070	12.0458
18.958	279.981		
	279.979	3.49975	12.2483
	279.938		
	279.933	3.49920	12.2444

Table 9. Results of roll moment of inertia determinations

Configuration	I_z ($kg \cdot m^2$)	$\Delta I_z / I_z$ (%)
1. Fixture + spacecraft	271.49	0.092
2a. Fixture as measured	77.547	0.212
2b. Increment for fixture with spacecraft*	0.045	
3. Spacecraft	193.90	0.154

*Longer bolts were used for attaching weight increments.

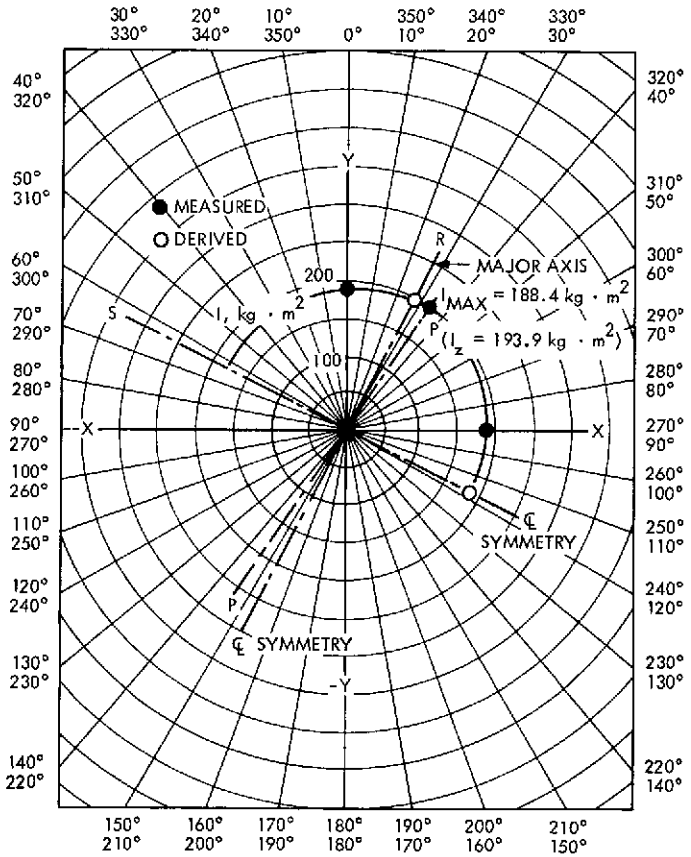

Fig. 1. Helios prototype spacecraft-inertia ellipse in X-Y plane

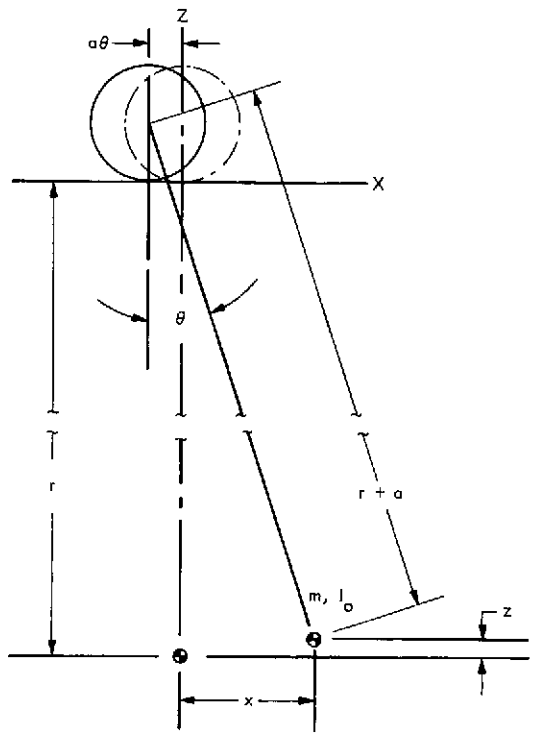

Fig. 2. Geometry of pendulous support

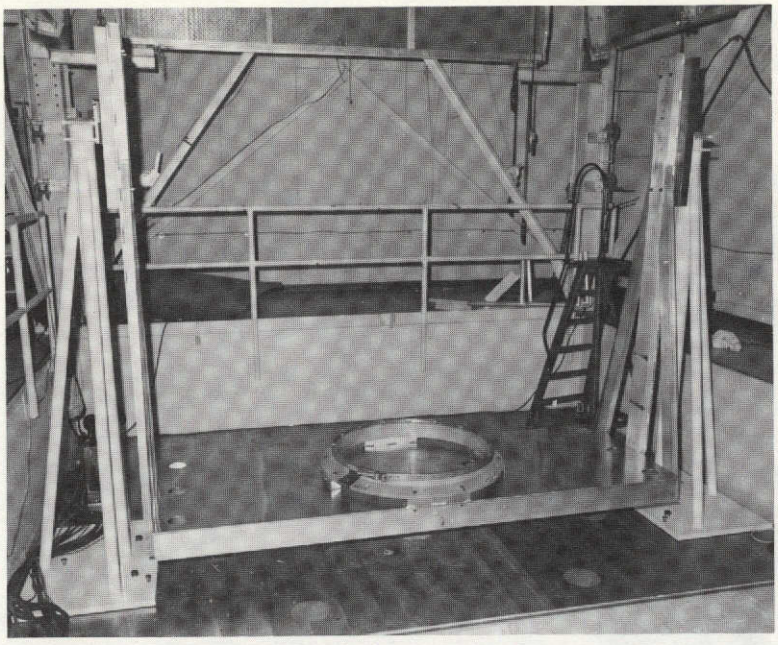

Fig. 3. Pendulous support for spacecraft

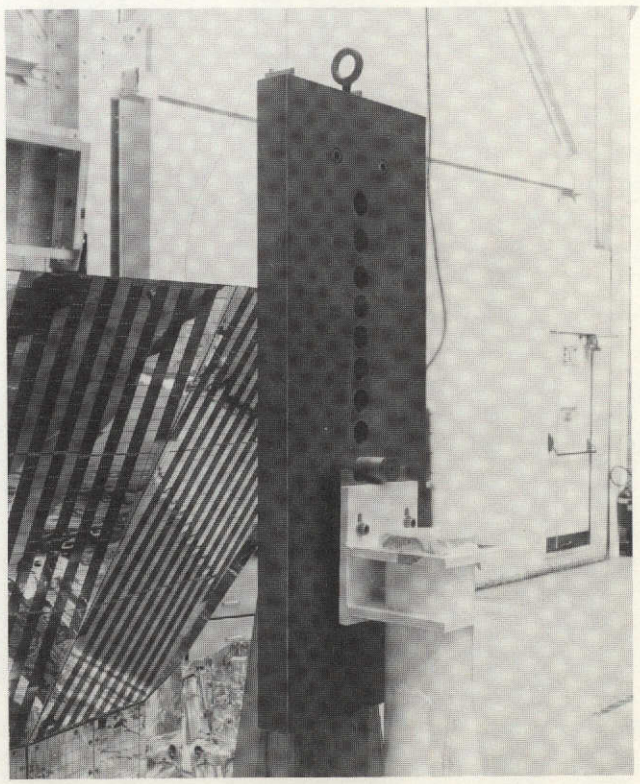

Fig. 4. Cradle ballast weight with optional positions for pivot pin (symmetrical about cradle centerplane)

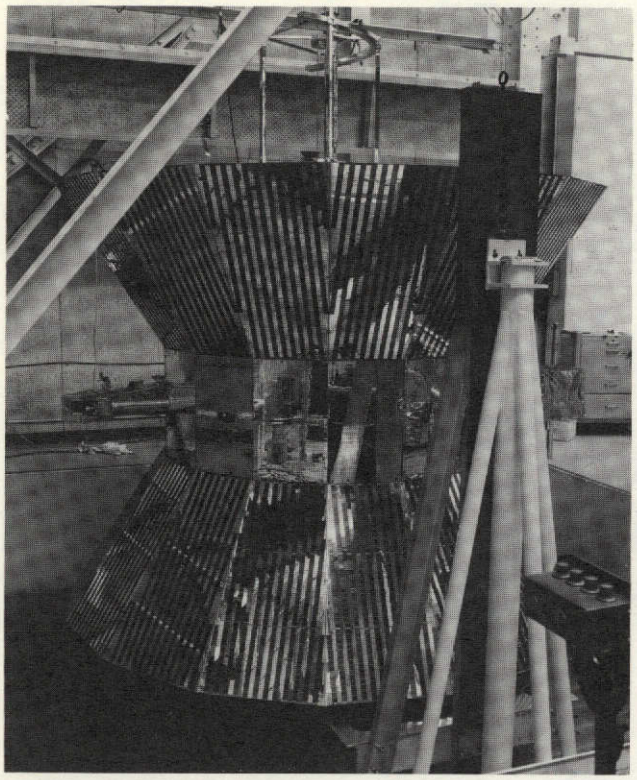

Fig. 5. Spacecraft on cradle with pins in hole "J" (see Fig. 8)

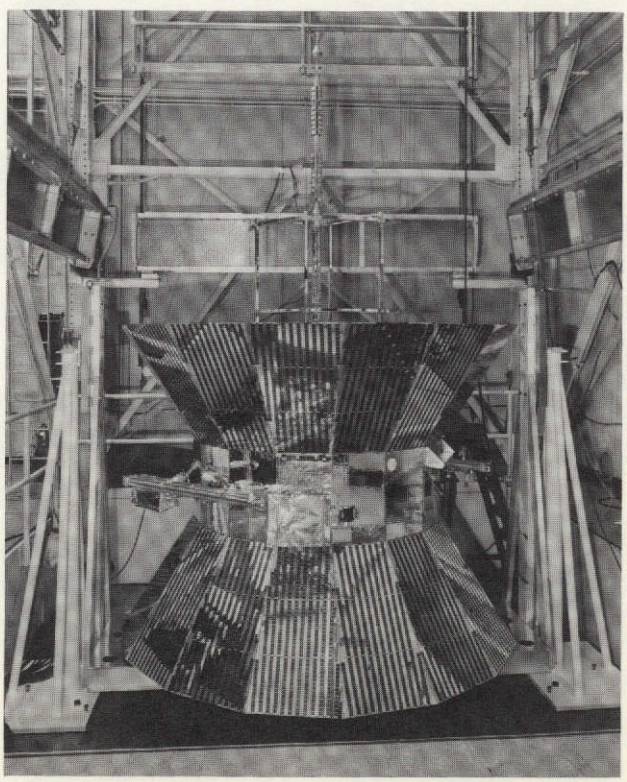

Fig. 6. Frontal view of spacecraft on cradle

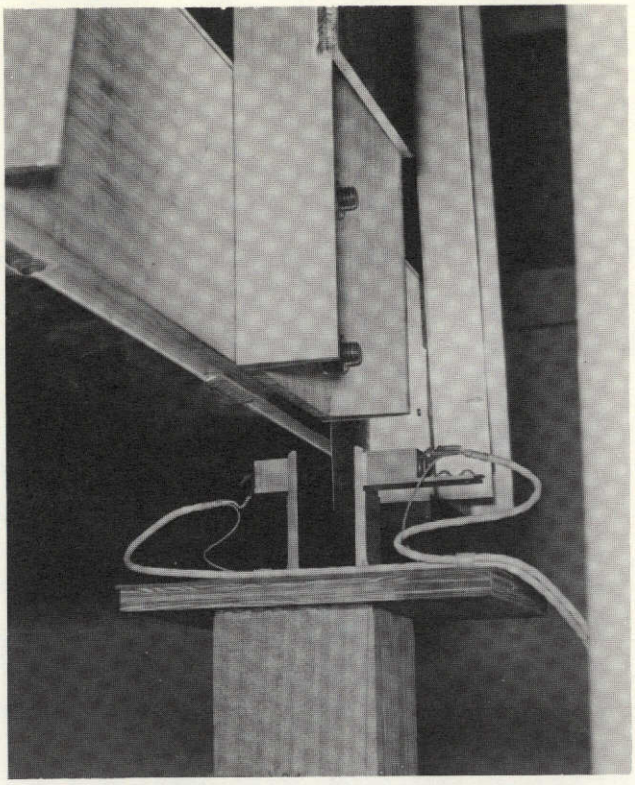

Fig. 7. Photoelectric sensor in place under cradle

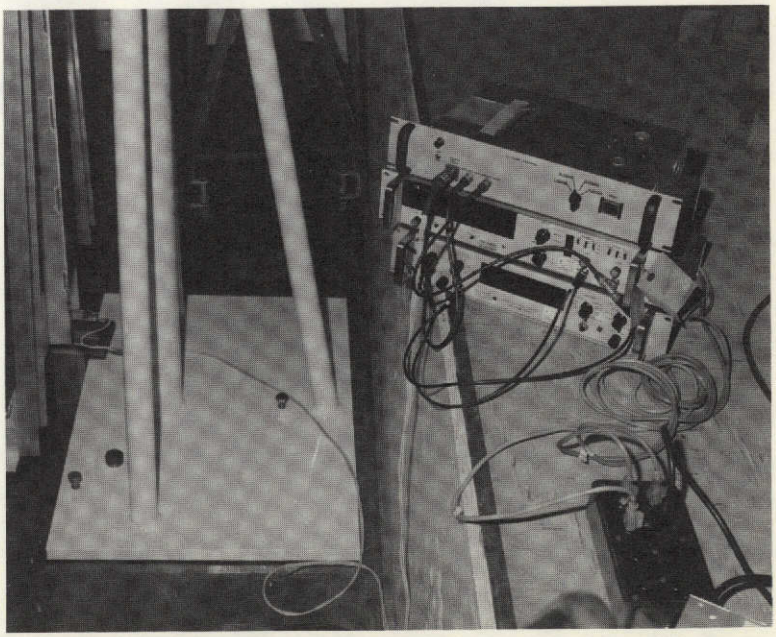

Fig. 8. Electronic counter/timer units

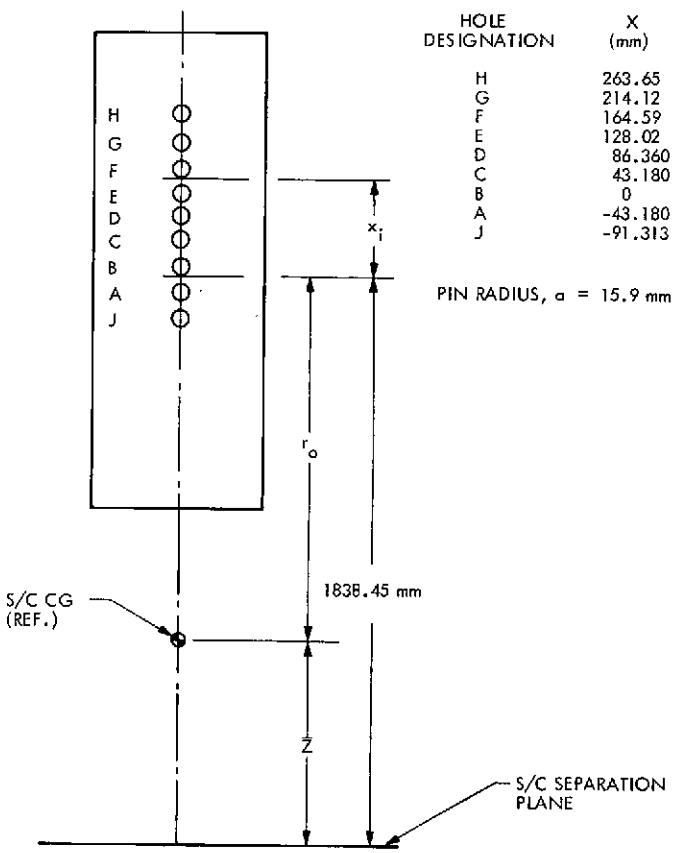

Fig. 9. Pivot-pin hole geometry relative to spacecraft separation plane

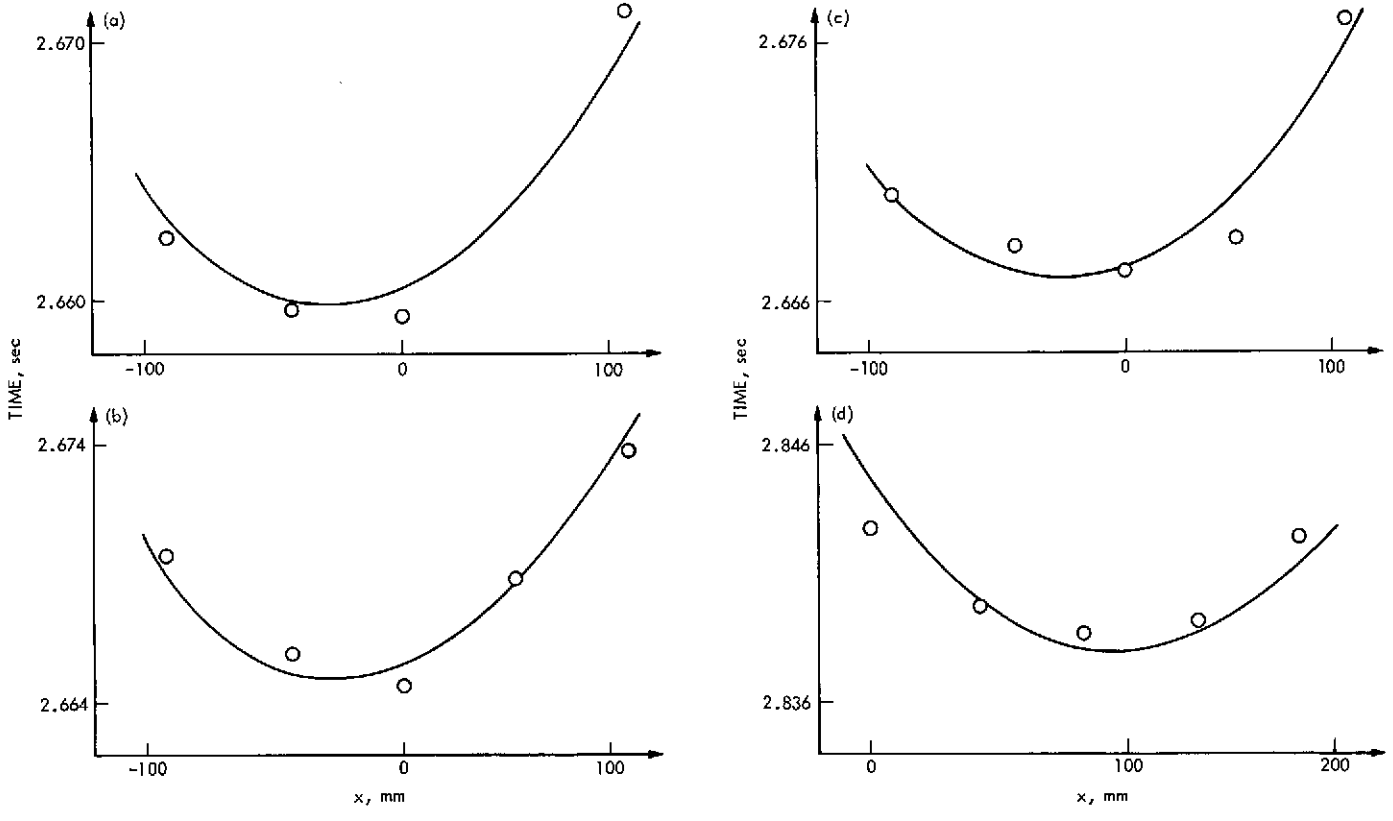

Fig. 10. Plots of T vs X for consistent r_o

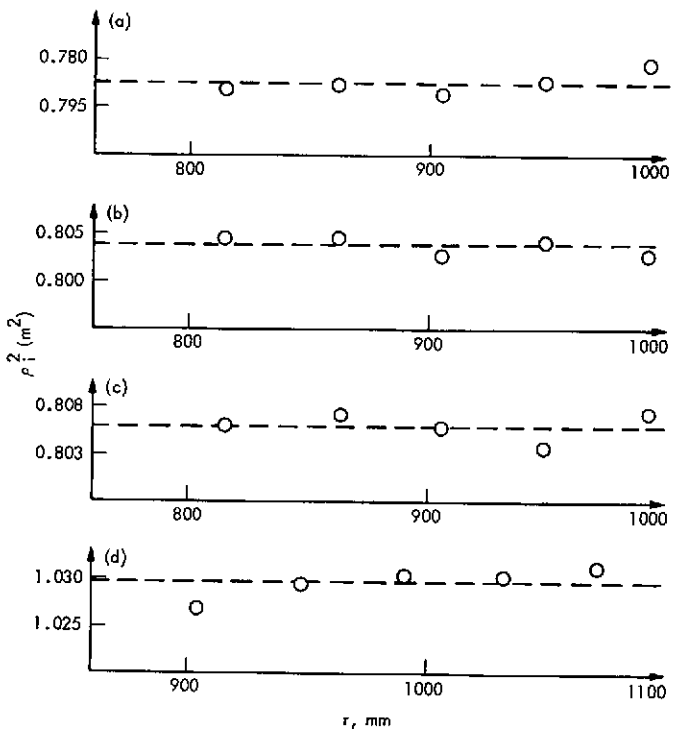

Fig. 11. Test scatter about statistically derived values of ρ_o^2

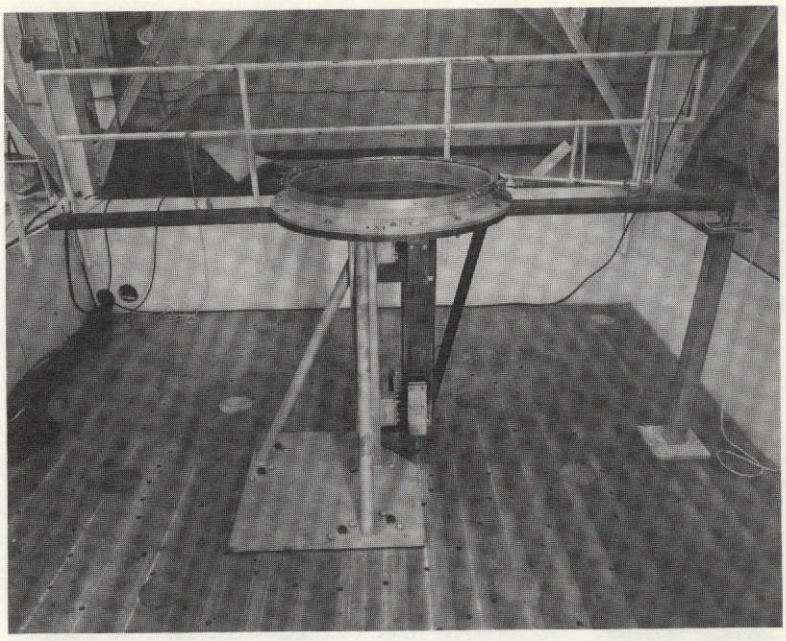

Fig. 12. Roll moment-of-inertia fixture with adapter and V-band installed

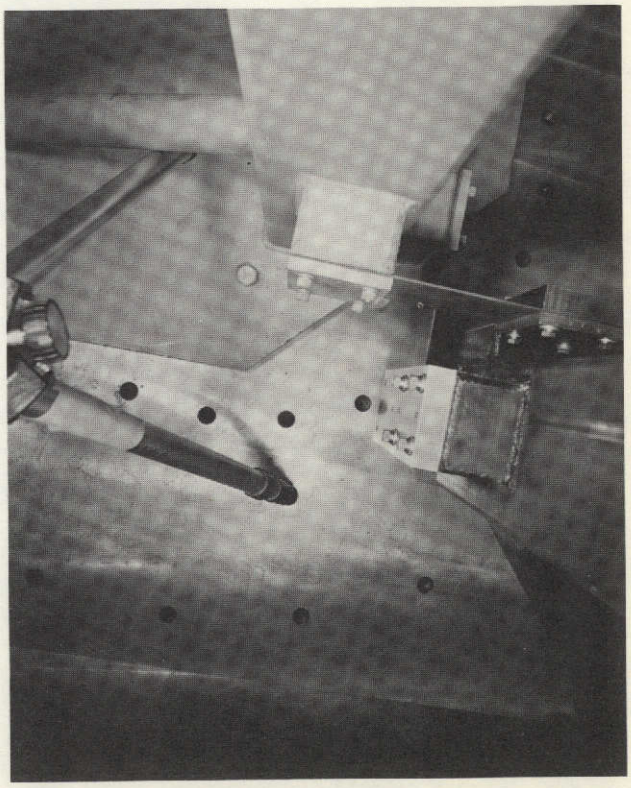

Fig. 13. Lower flexure-pivot assembly as viewed from above

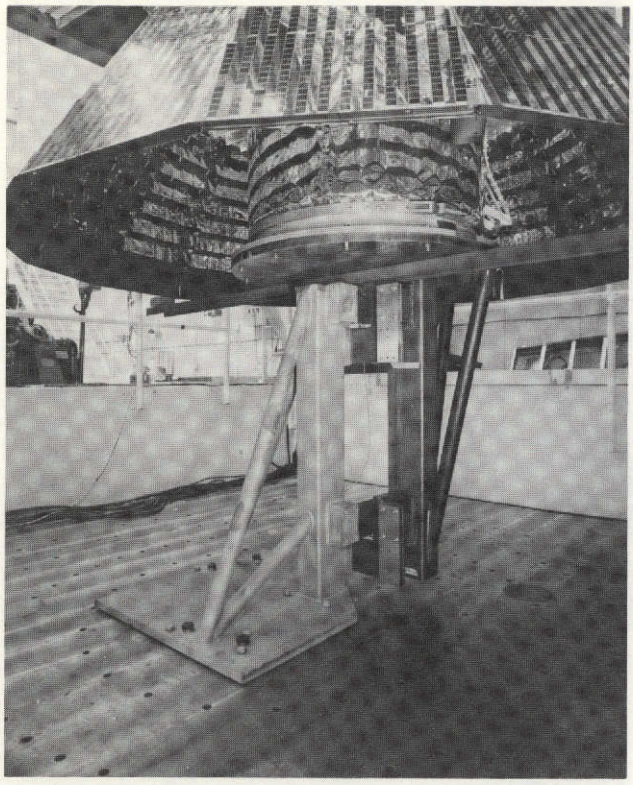

Fig. 14. Installation view of spacecraft on roll moment-of-inertia fixture

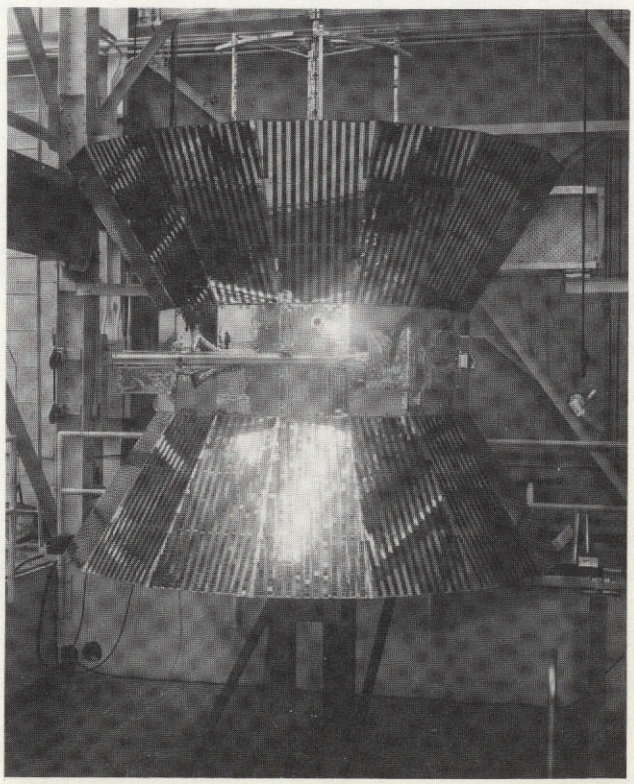

Fig. 15. Overall view — spacecraft on roll moment-of-inertia fixture

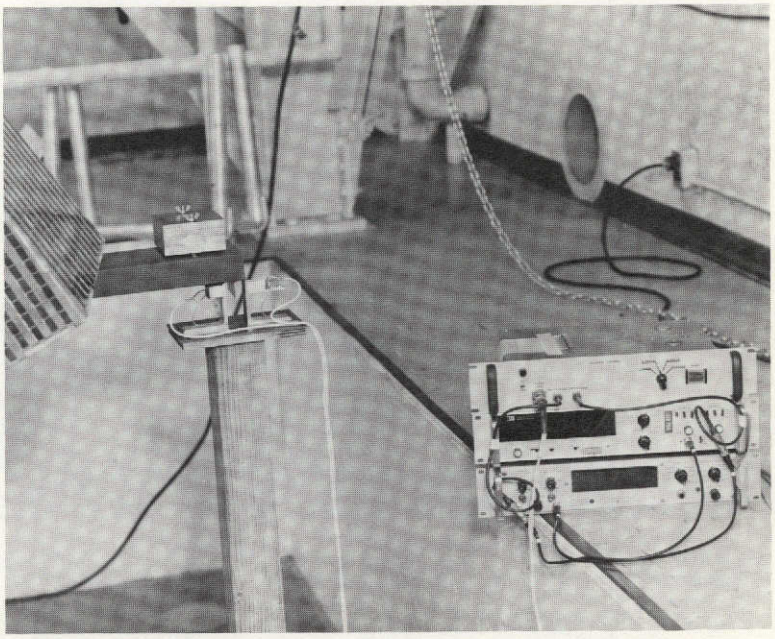

Fig. 16. Installation of incremental test weights on transverse arm

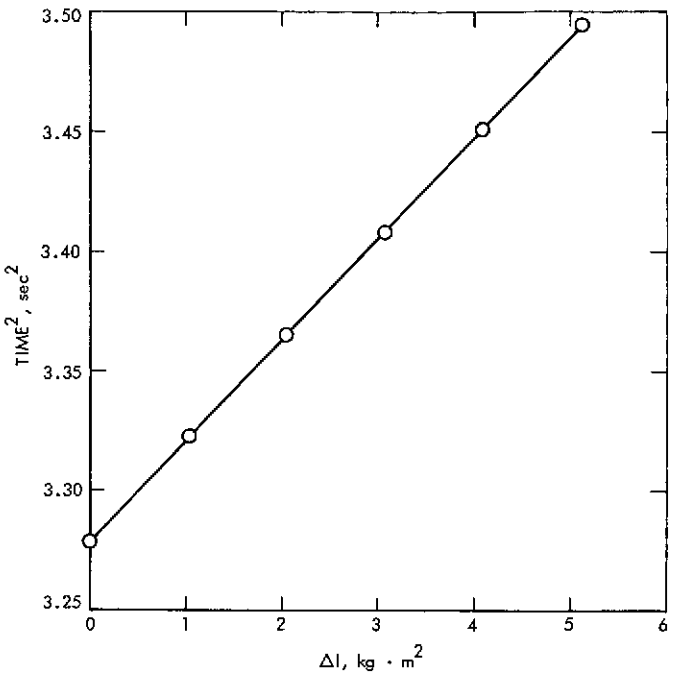

Fig. 17. Plot of T^2 vs ΔI for bare fixture

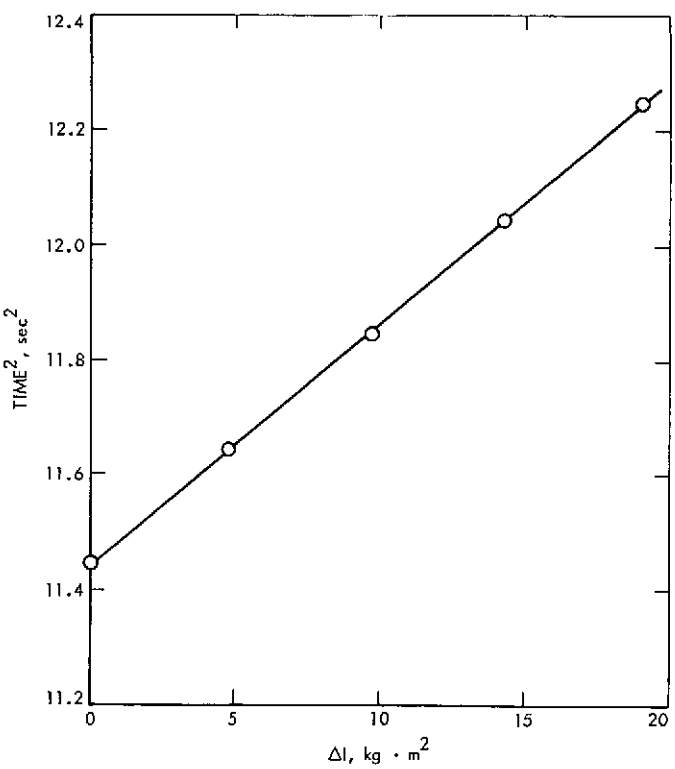

Fig. 18. Plot of T^2 vs ΔI for fixture plus spacecraft

APPENDIX A

ERROR ANALYSES RELATED TO DEFINITION OF THE INERTIA ELLIPSE IN THE x-y PLANE

Weights

In the weighing operations involving fixturing, either of two load cells was used. These load cells were of 454-kg and 908-kg ratings, respectively. They were calibrated on a certified deadweight tester located in one of JPL's instrument laboratories to a read-out accuracy of 0.1 lb., or 0.046 kg. Let

W_F = weight of the cradle, plus adapter and V-band

W_h = weight of the hoisting sling

W_c = combined weight.

Then

$$W_F = W_c - W_h \tag{A.1}$$

$$\frac{dW_F}{W_F} = \frac{1}{W_F}\left(\frac{\partial W_F}{\partial W_c}\right) dW_c + \frac{1}{W_F}\left(\frac{\partial W_F}{\partial W_h}\right) dW_h \tag{A.2}$$

or

$$\left|\frac{\Delta W_F}{W_F}\right|_{max} = \left(\frac{W_c}{W_F}\right)\frac{\Delta W_c}{W_c} + \left(\frac{W_h}{W_F}\right)\frac{\Delta W_h}{W_h} \tag{A.3}$$

From the calibration data, the following estimates are made:

$$\frac{\Delta W_c}{W_c} = 0.0002; \qquad \frac{\Delta W_h}{W_h} = 0.001$$

Thus

$$\left|\frac{\Delta W_F}{W_F}\right|_{max} = 0.00035 \text{ or } 0.035\%$$

Now, let

W_T = total weight of fixture plus spacecraft plus hoisting sling

W_S = weight of spacecraft

$$W_S = W_T - W_F - W_h \tag{A.4}$$

By treatment similar to that accorded W_F, it can be shown that

$$\left|\frac{\Delta W_S}{W_S}\right|_{max} = \left(\frac{W_T}{W_S}\right)\frac{\Delta W_T}{W_T} + \left(\frac{W_F}{W_S}\right)\frac{\Delta W_F}{W_F} + \left(\frac{W_h}{W_S}\right)\frac{\Delta W_h}{W_h} \tag{A.5}$$

$$= 0.0010 \text{ or } 0.1\%$$

Static Determination of Fixture C.G.

In addition to errors in forces and distances, errors are also assumed in angular alignments, θ and ϕ, as depicted in the sketch below.

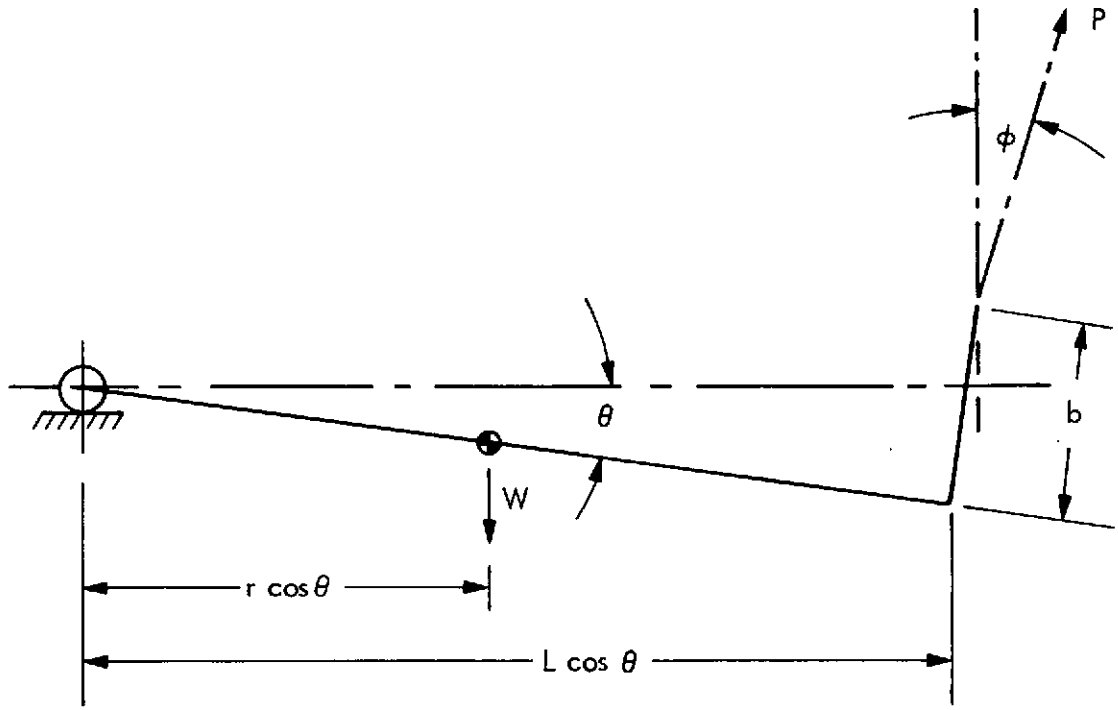

$$P = \frac{W}{\cos\phi} \quad \frac{r\cos\theta - a\theta}{L\cos\theta + b\sin\theta} \tag{A.6}$$

$$r = \frac{P}{W}\cos\phi\,(L + b\tan\theta) - \frac{a\theta}{\cos\theta} \tag{A.7}$$

$$\frac{dr}{r} = \frac{P}{r}\left(\frac{\partial r}{\partial P}\right)\frac{dP}{P} + \frac{W}{r}\left(\frac{\partial r}{\partial W}\right)\frac{dW}{W}$$

$$+ \frac{L}{r}\left(\frac{\partial r}{\partial L}\right)\frac{dL}{L} + \frac{b}{r}\left(\frac{\partial r}{\partial b}\right)\frac{db}{b} + \frac{a}{r}\left(\frac{\partial r}{\partial a}\right)\frac{da}{a}$$

$$+ \frac{\theta}{r}\left(\frac{\partial r}{\partial \theta}\right)\frac{d\theta}{\theta} + \frac{\phi}{r}\left(\frac{\partial r}{\partial \phi}\right)\frac{d\phi}{\phi} \tag{A.8}$$

$$\frac{\partial r}{\partial P} = \frac{\cos\phi}{W}(L + b\tan\theta)$$

$$\frac{\partial r}{\partial W} = -\frac{P\cos\phi}{W^2}(L + b\tan\theta)$$

$$\frac{\partial r}{\partial L} = \frac{P}{W}\cos\phi$$

$$\frac{\partial r}{\partial b} = \frac{P}{W}\cos\phi\tan\theta$$

$$\frac{\partial r}{\partial a} = -\frac{\theta}{\cos\theta}$$

$$\frac{\partial r}{\partial \theta} = \frac{Pb}{W}\cos\phi\sec^2\theta - \frac{a}{\cos\theta}(1 - \theta\tan\theta)$$

$$\frac{\partial r}{\partial \phi} = \left(-\frac{P}{W}\sin\phi\right)\left(L + b\tan\theta\right)$$

Here,

P = 186.71 kg (less V-band)

W = 417.72 - 7.54 = 410.18 kg (less V-band)

L = 2.169 m

b = 0.583 m

θ = ±0°3' (0.00087 rad.)

ϕ = ±0°30' (0.0087 rad.)

a = 0.0159 m

r = 0.9041 m

Then

$$\frac{\Delta r}{r} = 1.09\,\frac{\Delta P}{P} + 1.09\,\frac{\Delta W}{W} + 1.09\,\frac{\Delta L}{L}$$

with

$$\frac{\Delta P}{P} = 0.0007; \quad \frac{\Delta W}{W} = 0.00035; \quad \frac{\Delta L}{L} = 0.0006;$$

$$\frac{\Delta r}{r} = 0.0018, \text{ or } 0.18\%; \quad \Delta r = \pm 4 \text{ mm}$$

"Least Squares" Determination of the Radii of Gyration and Center of Gravity for the x-x, y-y and p-p Axes

From Eq. (1.15), the period T is given by

$$T = \frac{2\pi}{g}\sqrt{\frac{r^2 + \rho_o^2}{r + a}}$$

where a and g are known and the distance, r, from pin support to the system c.g. is given by

$$r = r_o + x$$

r_o is a reference length here, equal to the distance from the base of "Pin B" to the center of gravity, and x corresponds to increments on r_o to the different pin holes on the fixture.

The distance, r, from pin support to the c.g. was varied and the corresponding periods noted. The radius of gyration ρ_o^2 is first determined from the minimum value of T in a plot of T versus x. The following procedure determines the center of gravity position r_o and radius of gyration ρ_o^2 for the best fit of the experimental data.

To this end, the mean square error

$$\sigma^2 = \frac{1}{n}\sum_{i=1}^{n}\left(T_i - \frac{2\pi}{g}\sqrt{\frac{r_i^2 + \rho_o^2}{r_i + a}}\right)^2$$

where

$$r_i = r_o + x_i$$

is minimized with respect to r_o and ρ_o^2.

In order to simplify the algebra, the following was considered:

$$T_i^2 = \frac{4\pi^2}{g}\frac{\left(r_i^2 + \rho_o^2\right)}{r_i + a}, \qquad r_i = r_o + x_i$$

with

$$\frac{T^2}{4\pi^2/g} = D$$

Then

$$D_i = \frac{r_i^2 + \rho_o^2}{r_i + a}$$

$$D_i + 2a = (r_o + a + x_i) + \frac{\rho_o^2 + a}{r_o + a + x_i}$$

Put

$$R = r_o + a; \qquad B = \rho_o^2 + a^2; \qquad E_i = D_i + 2a$$

Then

$$E_i = R + x_i + \frac{B}{R + x_i}$$

and the mean square error

$$\sigma^2 = \frac{1}{n}\sum_{i=1}^{n} \left\{ E_i - \left[(R + x_i) + \frac{B}{R + x_i} \right] \right\}^2$$

is now considered.

The minimization with respect to R and B results in two nonlinear, simultaneous equations which are very difficult to solve. The problem is linearized by considering small increments on initial values (very close approximations) for R and B. Let

$$R = R_o + \alpha; \qquad B = B_o + \beta$$

and

$$R = R_o (1 + \zeta), \qquad B = R_o^2 (\bar{B}_o + \eta)$$

where R_o and B_o are the close approximations to R and B and

$$\zeta = \alpha/R_o, \qquad \eta = \beta/R_o^2, \qquad \bar{B}_o = B_o/R_o^2$$

then

$$\sigma^2 = \frac{1}{n}\sum_{i=1}^{n}\left\{E_i - \left[R_o + \alpha + x_i\right] - \frac{B_o + \beta}{R_o + \alpha + x_i}\right\}^2 \qquad \text{(A.9)}$$

$$\frac{\sigma^2}{R_o} = \frac{1}{n}\sum_{i=1}^{n}\left\{\bar{E}_i - \left[1 + \zeta + \bar{x}_i\right] - \frac{\bar{B}_o + \eta}{1 + \zeta + \bar{x}_i}\right\}^2$$

where

$$\bar{E}_i = E_i/R_o; \qquad \bar{x}_i = x_i/R_o$$

$$\frac{\sigma^2}{R_o} = \frac{1}{n}\sum_{i=1}^{n}\left\{\bar{E}_i - (1 + \bar{x}_i) - \zeta - \frac{(\bar{B}_o + \eta)}{(1 + \bar{x}_i)}\left(1 + \frac{\zeta}{i + \bar{x}_i}\right)^{-1}\right\}^2$$

Then, neglecting terms of order ζ^2:

$$\frac{\sigma^2}{R_o} = \frac{1}{n}\sum_{i=1}^{n}\left\{\bar{E}_i - (1 + \bar{x}_i) - \frac{\bar{B}_o}{(1 + \bar{x}_i)} - \left[1 - \frac{\bar{B}_o}{(1 + \bar{x}_i)^2}\right]\zeta - \frac{\eta}{(1 + \bar{x}_i)}\right\}^2 \qquad \text{(A.10)}$$

or

$$\frac{\sigma^2}{R_o} = \frac{1}{n}\sum_{i=1}^{n}(a_i + b_i\zeta + c_i\eta)^2 \qquad \text{(A. 11)}$$

where

$$a_i = \bar{E}_i - (1 + \bar{x}_i) - \frac{\bar{B}_o}{(1 + \bar{x}_i)}$$

$$b_i = \frac{\bar{B}_o}{(1 + \bar{x}_i)^2} - 1$$

$$c_i = \frac{-1}{(1 + \bar{x}_i)}$$

Differentiating Eq. (A. 11) with respect to ζ

$$\frac{\partial}{\partial\zeta}\left(\frac{\sigma^2}{R_o}\right) = \frac{1}{n}\sum_{i=1}^{n} 2b_i\,(a_i + b_i\zeta + c_i\eta)$$

and since

$$\frac{\partial}{\partial\zeta}\left(\frac{\sigma^2}{R_o}\right) = 0$$

for a minimum

$$\Longrightarrow \quad \zeta\sum_{i=1}^{n} b_i^2 + \eta\sum_{i=1}^{n} b_i\,c_i + \sum_{i=1}^{n} b_i\,a_i = 0 \qquad \text{(A. 12)}$$

Similarly for η:

$$\frac{\partial}{\partial \eta}\left(\frac{\sigma^2}{R_o}\right) = \frac{1}{n}\sum_{i=1}^{n} 2c_i\,(a_i + b_i\zeta + c_i\eta)$$

and

$$\frac{\partial}{\partial \eta}\left(\frac{\sigma^2}{R_o}\right) = 0$$

$$\Longrightarrow \quad \zeta\sum_{i=1}^{n} b_i c_i + \eta\sum_{i=1}^{n} c_i^{\,2} + \sum_{i=1}^{n} a_i c_i = 0 \qquad \text{(A. 13)}$$

Solving for ζ and η: from (A. 12),

$$\eta = \frac{-1}{\sum b_i\, c_i}\left(\sum b_i\, a_i + \zeta \sum b_i^{\,2}\right) \qquad \text{(A. 14)}$$

and from Eqs. (A. 13) and (A. 14)

$$\zeta = \frac{\sum a_i\, b_i \sum c_i^{\,2} - \sum a_i\, c_i \sum b_i\, c_i}{\left(\sum b_i\, c_i\right)^2 - \sum b_i^{\,2} \sum c_i^{\,2}} \qquad \text{(A. 15)}$$

Thus, knowing the values of ζ and η, R and B are found from the relationships

$$R = R_o + \alpha \qquad \text{and} \qquad B = B_o + \beta$$

This was further developed into the following iterative scheme suitable for a small computer program.

Values of ζ and η are calculated for the close approximations to R and B, R_o and B_o respectively, and the values of R and B calculated therefrom are substituted into the expressions for ζ and η as new close approximations. The new values of ζ and η are then used to find new values of R and B and the cycle repeated until sufficient convergence is achieved.

That is:

$$R_o^{(j+1)} = R_o^{(j)} + \alpha^{(j)}$$

$$B_o^{(j+1)} = B_o^{(j)} + \beta^{(j)}$$

A small computer program was written. Convergence to numerically acceptable values of r_o and ρ_o^2 was realized typically within five to six iterations.

Radii of Gyration with Consistent C. G. Location

An additional step was taken following the determination of the center of gravity location and radius of gyration of each of the three axes tested (i.e., x-x axis, y-y axis and p-p axis of the spacecraft and fixture). This step makes use of the fact that the center of gravity position should be the same for all three axes. The values for r_o were close but not exactly the same for the three axes and, accordingly, an average value of the three values of r_o was taken to give a consistent value of r_o. This value of r_o was then used to compute new values of ρ_o^2 for each of the three axes as follows: from before,

$$D = (g/4\pi^2)T^2 \qquad \text{and} \qquad D = \frac{\rho_o^2 + r^2}{r + a}; \qquad r = r_o + x$$

Define the radius of gyration ρ_o for each location of the axis of rotation:

$$\rho_i^2 = (r_i + a)\, D_i - r_i^2 \tag{A. 16}$$

$$i = 1, \cdots, n$$

Then ρ_o^2 is the mean of the n values of ρ_i^2

$$\rho_o^2 = \frac{1}{n}\left(\sum_{i=1}^{n}(r_i + a)\, D_i - \sum_{i=1}^{n} r_i^2\right) \qquad (A.17)$$

which can be written as Eq. (1.21).

Finally, the variance S^2 on ρ_o^2 is calculated by

$$S^2 = \frac{1}{n-1}\sum_{i=1}^{n}\left(\rho_o^2 - (r_i + a)\, D_i + r_i^2\right)^2 \qquad (A.18)$$

for the best fit.

A similar technique was used in the case of the bare fixture where the center of gravity value calculated from the static test was used in preference to the one determined by experiment and best fit. In all cases the differences in the radii of gyration calculated by the best fit program and the consistent C.G. location technique were small (0.03% in the worst case). The consistent C.G. location technique using Eq. (1.21) is believed to give the best determination of the radii of gyration.

Extraction of Spacecraft Inertial Properties

The variances on the radii of gyration of the spacecraft alone were then calculated from:

$$S_S^2 = (1 + M_F/M_S)\, S_T^2 + M_F/M_S\, S_F^2$$

where

M_F = mass of fixture

M_S = mass of spacecraft

S_F^2 = variance on fixture radius of gyration

S_T^2 = variance on fixture + spacecraft radius of gyration

S_S^2 = variance on spacecraft radius of gyration

The error estimates on the spacecraft moments of inertia are then given by

$$I_S = M_S \rho_o{}^2{}_S$$

and

$$\left(\frac{\Delta I_S}{I_S}\right)_{max} = \frac{\Delta M_S}{M_S} + \frac{\Delta \rho_o{}^2}{\rho_o{}^2}$$

or

$$\frac{\Delta I_S}{I_S} = \frac{\Delta M_S}{M_S} + \frac{S_S}{\rho_{oS}^2} \qquad \text{(A. 20)}$$

N. B. $\Delta I_S/I_S$ is an estimate of the error. $\Delta I_S/I_S$ is made up of an absolute error on M_S and a statistical error estimate on ρ_{oS}^2 and therefore not strictly the maximum absolute error.

Axis	ρ_o^2 (M^2)	S_S (M^2)	I (kg · m^2)	$\frac{\Delta I}{I}$ (%)
x-x	0.5201	0.0026	181.7	0.61
y-y	0.5341	0.0022	186.6	0.52
p-p	0.5389	0.0031	188.3	0.67

Finally, from Eq. (1.25)

$$r_{oS} = M_F/M_S\,(r_{oT} - r_{oS}) + r_{oT}$$

$$\Longrightarrow \quad r_{oS} = 0.9093 \text{ m} \qquad \text{and} \qquad \overline{Z} = 1838.45 \text{ mm}$$

The Inertia Ellipse

From Eq. (1.29)

$$\frac{dU_{xy}}{U_{xy}} = \frac{1}{U_{xy}}\left(\frac{\partial U_{xy}}{\partial I_x}\right) dI_x + \frac{1}{U_{xy}}\left(\frac{\partial U_{xy}}{\partial I_y}\right) dI_y$$

$$+ \frac{1}{U_{xy}}\left(\frac{\partial U_{xy}}{\partial I_p}\right) dI_p + \frac{1}{U_{xy}}\left(\frac{\partial U_{xy}}{\partial \alpha}\right) d\alpha \qquad \text{(A.21)}$$

where

$$\frac{\partial U_{xy}}{\partial I_x} = \frac{1}{2}\,\text{ctn}\,\alpha = 0.3340$$

$$\frac{\partial U_{xy}}{\partial I_y} = \frac{1}{2}\tan\alpha = 0.7483$$

$$\frac{\partial U_{xy}}{\partial I_p} = -\frac{1}{\sin 2\alpha} = -1.082$$

$$\frac{\partial U_{xy}}{\partial \alpha} = (I_y - I_x) - 2U_{xy} \operatorname{ctn} 2\alpha = 0$$

Thus

$$\frac{\Delta U_{xy}}{U_{xy}} = 0.3340 \left(\frac{I_x}{U_{xy}}\right) \frac{\Delta I_x}{I_x} + 0.7483 \left(\frac{I_y}{U_{xy}}\right) \frac{\Delta I_y}{I_y}$$

$$- 1.082 \left(\frac{I_p}{U_{xy}}\right) \frac{\Delta I_p}{I_p}$$

$$= -0.1072 - 0.2102 + 0.3951$$

$$= 0.0777$$

For the error in ϕ,

$$\frac{d\phi}{\phi} = \frac{1}{\phi} \left(\frac{\partial \phi}{\partial U_{xy}}\right) dU_{xy} + \frac{1}{\phi} \left(\frac{\partial \phi}{\partial I_x}\right) dI_x$$

$$+ \frac{1}{\phi} \left(\frac{\partial \phi}{\partial I_y}\right) dI_y \qquad \text{(A.22)}$$

From Eq. (1.31)

$$\frac{\partial \phi}{\partial U_{xy}} = \frac{-(I_x - I_y)}{(I_x - I_y)^2 + 4U_{xy}^2}$$

$$\frac{\partial \phi}{\partial I_x} = -\frac{\partial \phi}{\partial I_y} = \frac{U_{xy}}{(I_x - I_y)^2 + 4U_{xy}^2}$$

Thus

$$\frac{\Delta\phi}{\phi} = 0.052 \qquad \text{or} \qquad \Delta\phi = \pm 1.4^\circ$$

Finally,

$$\frac{dI_r}{I_r} = \frac{1}{I_r}\left(\frac{\partial I_r}{\partial I_x}\right) dI_x + \frac{1}{I_r}\left(\frac{\partial I_r}{\partial I_y}\right) dI_y$$

$$+ \frac{1}{I_r}\left(\frac{\partial I_r}{\partial U_{xy}}\right) dU_{xy} + \frac{1}{I_r}\left(\frac{\partial I_r}{\partial \phi}\right) d\phi \qquad \text{(A.23)}$$

From Eq. (1.28)

$$\frac{\partial I_r}{\partial I_x} = \cos^2\phi\ ; \qquad \frac{\partial I_r}{\partial I_y} = \sin^2\phi$$

$$\frac{\partial I_r}{\partial U_{xy}} = \sin 2\phi; \qquad \frac{\partial I_r}{\partial \phi} = -2U_{rs} = 0$$

$$\frac{\Delta I_r}{I_r} = 0.65\%; \qquad \frac{\Delta I_s}{I_s} = 0.47\%$$

Errors in Spacecraft C.G. Determination

From Eq. (1.25),

$$r_{oS} = \frac{M_F}{M_S}(r_{oT} - r_{oF}) + r_{oT}$$

$$dr_{oS} = \frac{\partial r_{oS}}{\partial M_F} dM_F + \frac{\partial r_{oS}}{\partial M_S} dM_S + \frac{\partial r_{oS}}{\partial r_{oT}} dr_{oT} + \frac{\partial r_{oS}}{\partial r_{oF}} dr_{oF}$$

$$\left|\Delta r_{oS}\right|_{max} = \frac{M_F}{M_S}(r_{oT} - r_{oF})\frac{\Delta M_F}{M_F} + \frac{M_F}{M_S}(r_{oT} - r_{oF})\frac{\Delta M_S}{M_S}$$

$$+ \left(\frac{M_F}{M_S} + 1\right)\Delta r_{oT} + \frac{M_F}{M_S}\Delta r_{oF} \qquad (A.24)$$

Here,

M_F = 416.80 kg

M_S = 350.08 kg

r_{oT} = 906.5 mm (average value from Table 6)

r_{oF} = 904.2 mm (from static test)

$\frac{\Delta M_F}{M_F}$ = 0.0035

$\frac{\Delta M_S}{M_S}$ = 0.001

Δr_{oT} = 6.6 mm (max. deviation from Table 6)

Δr_{oF} = 4.4 mm (from error analysis of static test)

and

Δr_{oS} = ±19.3 mm

APPENDIX B

ROLL MOMENT OF INERTIA DETERMINATION AND ERROR ANALYSIS

Roll Moment of Inertia Determination

From Eqs. (2.3 and (2.4) we have

$$T^2 = T_o^2 + m\Delta I \tag{B.1}$$

where

$$m = \frac{T_o^2}{I_o} \tag{B.2}$$

The period, T_o, for zero mass increment and the slope m can be determined statistically from a least squares fit of the test data to a plot of T^2 versus ΔI.

The mean square error is given by

$$\sigma^2 = \frac{1}{n}\sum_{i=1}^{n}\left(T_i^2 - T_o^2 - m\Delta I_i\right)^2 \tag{B.3}$$

Minimizing with respect to m and T_o^2

$$\frac{\partial \sigma^2}{\partial m} = 0 = \frac{1}{n}\sum_{i=1}^{n} 2\left(T_i^2 - T_o^2 - m\Delta I_i\right)\left(-\Delta_i\right)$$

Then,

$$T_o^2 \sum \Delta I_i + m \sum (\Delta I_i)^2 = \sum \Delta I_i \, T_i^2 \tag{B.4}$$

and

$$\frac{\partial \sigma^2}{\partial T_o^2} = 0 = \frac{1}{n} \sum 2 \left(T_i^2 - T_o^2 - m\Delta I_i \right)(-1)$$

which gives

$$T_o^2 \, n + m \sum \Delta I_i = \sum T_i^2 \tag{B.5}$$

Dividing Eqs. (B.4) and (B.5) by m:

$$\frac{T_o^2}{m} \sum \Delta I_i - \frac{1}{m} \sum \Delta I_i \, T_i^2 = - \sum (\Delta I_i)^2 \tag{B.6}$$

$$\frac{T_o^2}{m} n - \frac{1}{m} \sum T_i^2 = - \sum \Delta I_i \tag{B.7}$$

From Eq. (B.6),

$$\frac{1}{m} = \frac{1}{\sum \Delta I_i \, T_i^2} \left(\sum (\Delta I_i)^2 + \frac{T_o^2}{m} \sum \Delta I_i \right) \tag{B.8}$$

and substituting Eq. (B.8) into Eq. (B.7) it is found that

$$\frac{T_o^2}{m} = I_o = \frac{\sum T_i^2 \sum (\Delta I_i)^2 - \sum \Delta I_i \sum T_i^2 \Delta I_i}{n \sum \Delta I_i \, T_i^2 - \sum T_i^2 \sum \Delta I_i} \tag{B.9}$$

Error Analysis

The variance σ^2 on the period squared T^2 is given by:

$$\sigma^2 = \frac{1}{n-1} \sum \left(T^2_{fit} - T^2_{measured} \right)^2 \tag{B.10}$$

The slope and intercept variances, σ_m^2 and $\sigma_{T_o^2}^2$ respectively, then follow:

$$\sigma^2_m = \frac{\sigma^2}{\sum\left(\Delta I_i - \overline{\Delta I}\right)^2} \tag{B. 11}$$

$$\sigma^2_{T_o^2} = \frac{\sigma^2 \sum \left(\Delta I_i\right)^2}{n \sum \left(\Delta I_i - \overline{\Delta I}\right)^2} \tag{B. 12}$$

The variance on the roll moment of inertia I_o is given by:

$$I_o = \frac{T_o^2}{m}$$

$$\ell n\, I_o = \ell n\, T_o^2 - \ell n\, m$$

$$\left|\frac{\Delta I_o}{I_o}\right| \leq \left|\frac{\Delta T_o^2}{T_o^2}\right| + \left|\frac{\Delta m}{m}\right|$$

$$\left(\frac{\Delta I_o}{I_o}\right)_{max} = \frac{\Delta T_o^2}{T_o^2} + \frac{\Delta m}{m}$$

or

$$\frac{\sigma_{I_o}}{I_o} = \frac{\sigma_{T_o^2}}{T_o^2} + \frac{\sigma_m}{m} \tag{B. 13}$$

The error estimate on the roll moment of inertia of the spacecraft alone is then given by

$$\sigma^2_{I_{oS}} = \sigma^2_{I_{oT}} + \sigma^2_{I_{oF}} \tag{B. 14}$$

where subscripts are

S ≡ spacecraft

T ≡ spacecraft + fixture

F ≡ fixture alone.

APPENDIX C

MODEL TESTS AND ASSOCIATED ANALYSES

The objectives of the model tests were twofold:

(1) to acquire knowledge that could reflect to advantage in the design of the full-scale test fixturing.

(2) to assess the accuracy potential prior to start of fabrication of the full-scale fixturing.

The implementation of this model program was predicated on the assumption that the moments of inertia of prismatic bars representing "fixture" and "spacecraft" could be calculated with sufficient accuracy to serve as "absolute standards" for judging experimental accuracy.

Accordingly, bars of precision-ground tool steel were machined and drilled according to design requirements, and actual dimensions were checked to an accuracy of 0.003 mm by JPL's Inspection Department. The actual dimensions were used in calculations of ρ_o^2 of each element, with allowance for material removed for containing the pivot pin.

Figure C-1 is a view of the "fixture" simulator in place on its supporting structure, which provided appropriately spaced drill rods as the ways on which the pivot pin rode.

Figure C-2 shows the elements of the complete model; the combination of the two smaller bars represents the "spacecraft."

The test models were purposely designed so that they could be used as "reversible pendulums," and oscillation tests were conducted in both aspects. Actual weights of the model elements were measured on a certified gram balance.

The test data were processed in the same manner as that accorded the data of the full-scale tests. The results are summarized in Table C-1.

The experimentally determined value of the "fixture" I_o is in excellent agreement with the "actual" value, which was derived from a measured weight and a value of ρ_o^2 calculated from the bar geometry. The corresponding comparison for "fixture plus spacecraft" is not nearly as good,

suggesting some systematic inaccuracy that was not revealed by the statistical error analysis.

It is to be noted that, under the combined weight of "fixture" and "spacecraft," galling of the 4.8-mm (0.188-inch) diameter drill rod that served as the pivot pin was observed. This situation appeared to be relieved by using a plug gage of greater surface hardness. However, it is not certain that the problem was completely eliminated, as the bearing stresses under nominal "point contact" were very high. Any flattening of the pivot pin increases the pin radius, a, reduces the parameter, D_m, and hence the experimentally derived value of ρ_o^2. Thus the design of the full-scale fixturing provided for line contact of the pins on flat ways, although this ideal situation was not completely realized in the full-scale tests for reasons noted.

The error in the "spacecraft" moment of inertia shown in Table C-1 is, of course, magnified in the process of removing the "fixture" from "fixture plus spacecraft." Even so, an accuracy of better than 1% was achieved, demonstrating the high accuracy attainable by the method.

Table C-1. Comparisons of measured and "actual" inertial properties

1.	"Fixture"	
	Mass (kg)	4.622
	Experimentally determined I_o (kg m^2)	0.08456
	Estimated statistical test error	±0.23%
	"Actual" moment of inertia, I_o' (kg m^2)	0.08458
	Experimental error (%) based on I_o'	-0.03%
2.	"Fixture" plus "spacecraft"	
	Mass (kg)	8.587
	Experimentally determined I_o (kg m^2)	0.13270
	Estimated statistical test error	±0.24%
	"Actual" moment of inertia, I_o' (kg m^2)	0.13324
	Experimental error (%) based on I_o'	-0.40%
3.	"Spacecraft"	
	Mass (kg)	3.965
	Experimentally determined I_o (kg m^2)	0.04814
	Estimated statistical test error	±0.43%
	"Actual" moment of inertia, I_o' (kg m^2)	0.04852
	Experimental error (%) based on I_o'	-0.78%

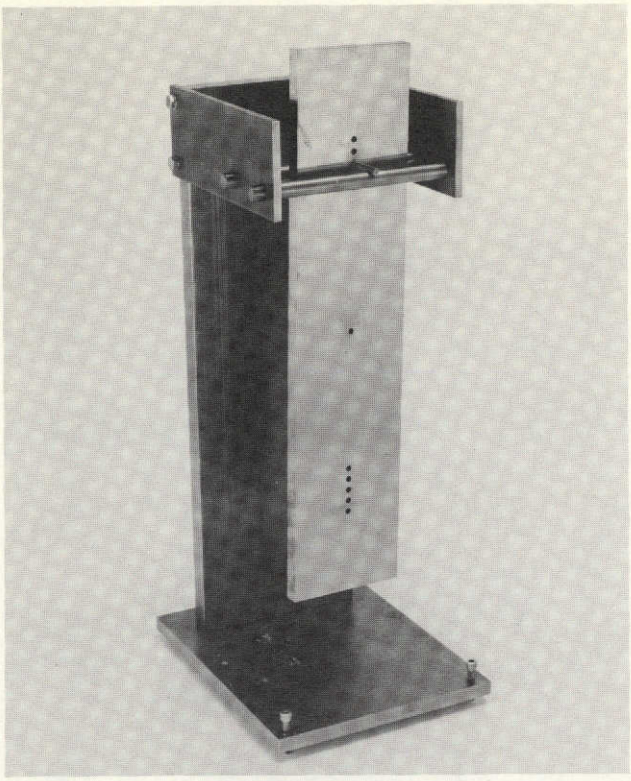

Fig. C-1. Model for test of radius-of-gyration measurement concept

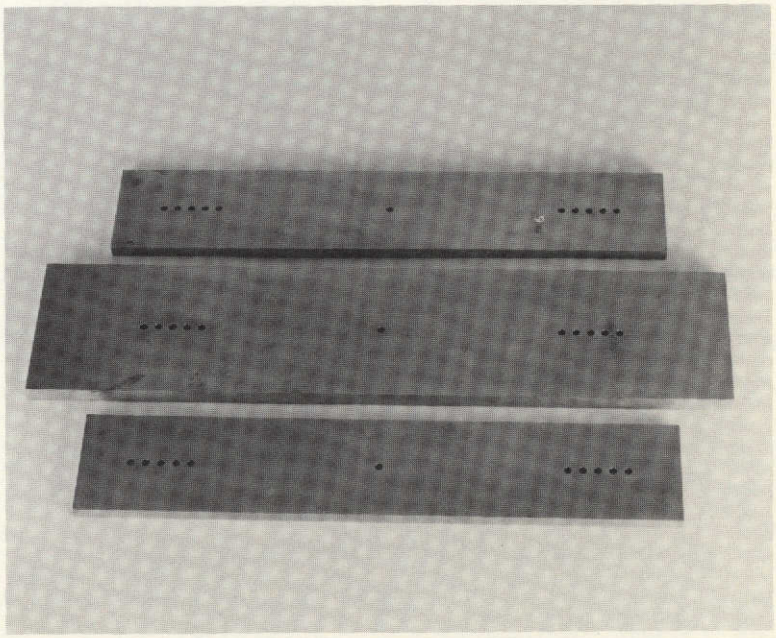

Fig. C-2. Elements of complete model

NASA—JPL—Coml., L. A. Calif.